Global satellite observations of column-averaged carbon dioxide and methane: The GHG-CCI XCO2 and XCH4 CRDP3 data set

M. Buchwitz, M. Reuter, O. Schneising, W. Hewson, R.G. Detmers, H. Boesch, O.P. Hasekamp, I. Aben, H. Bovensmann, J.P. Burrows, et al.

Global satellite observations of column-averaged carbon dioxide and methane: The GHG-CCI XCO_2 and XCH_4 CRDP3 data set

M. Buchwitz,[1], M. Reuter[1], O. Schneising[1], W. Hewson[2], R. G. Detmers[3], H. Boesch[2], O. P. Hasekamp[3], I. Aben[3], H. Bovensmann[1], J. P. Burrows[1], A. Butz[4], F. Chevallier[5], B. Dils[6], C. Frankenberg, [7, 12], J. Heymann[1], G. Lichtenberg[8], M. De Mazière[6], J. Notholt[1], R. Parker[2], T. Warneke[1], C. Zehner[9], D. W. T. Griffith[10], N. M. Deutscher[1, 10], A. Kuze[11], H. Suto[11], D. Wunch[12, #]

1. Institute of Environmental Physics (IUP), University of Bremen, Bremen, Germany.
2. University of Leicester, Leicester, United Kingdom.
3. SRON Netherlands Institute for Space Research, Utrecht, Netherlands.
4. Karlsruhe Institute of Technology (KIT), Karlsruhe, Germany.
5. Laboratoire des Sciences du Climat et de l'Environnement (LSCE), Gif-sur-Yvette, France.
6. Belgian Institute for Space Aeronomy (BIRA), Brussels, Belgium.
7. Jet Propulsion Laboratory (JPL), Pasadena, California, United States of America.
8. Deutsches Zentrum für Luft- und Raumfahrt (DLR), Oberpfaffenhofen, Germany.
9. European Space Agency (ESA), ESRIN, Frascati, Italy.
10. University of Wollongong, Wollongong, Australia.
11. Japan Aerospace Exploration Agency (JAXA), Tsukuba, Japan.
12. California Institute of Technology, Pasadena, California, United States of America.

#) Now at: University of Toronto, School of the Environment, Toronto, Canada.

**) Corresponding author: Michael Buchwitz, Institute of Environmental Physics (IUP), University of Bremen, FB1, Otto Hahn Allee 1, 28334 Bremen, Germany, Phone: +49-(0)421-218-62086, Fax: +49-(0)421-218-62070, E-mail: Michael.Buchwitz@iup.physik.uni-bremen.de.*

Abstract

Carbon dioxide (CO_2) and methane (CH_4) are the two most important greenhouse gases emitted by mankind. Better knowledge of the surface sources and sinks of these Essential Climate Variables (ECVs) and related carbon uptake and release processes is needed for important climate change related applications such as improved climate modelling and prediction. Some satellites provide near-surface-sensitive atmospheric CO_2 and CH_4 observations that can be used to obtain information on CO_2 and CH_4 surface fluxes. The goal of the GHG-CCI project of the European Space Agency's (ESA) Climate Change Initiative (CCI) is to use satellite data to generate atmospheric CO_2 and CH_4 data products meeting demanding GCOS (Global Climate Observing System) greenhouse gas (GHG) ECV requirements. To achieve this, retrieval algorithms are regularly being improved followed by annual data reprocessing and analysis cycles to generate better products in terms of extended time series and continuously improved data quality. Here we present an overview about the latest GHG-CCI data set called Climate Research Data Package No. 3 (CRDP3) focusing on the GHG-CCI core data products, which are column-averaged dry-air mole fractions of CO_2 and CH_4, i.e., XCO_2 and XCH_4, as retrieved from SCIAMACHY/ENVISAT and TANSO/GOSAT satellite radiances covering the time period end of 2002 to end of 2014. We present global maps and time series including initial validation results obtained by comparisons with Total Carbon Column Observing Network (TCCON) ground-based observations. We show that the GCOS requirements for systematic error (< 1 ppm for XCO_2, < 10 ppb for XCH_4) and long-term stability (< 0.2 ppm/year for XCO_2, < 2 ppb/year for XCH_4) are met for nearly all products (an exception is SCIAMACHY methane especially since 2010). For XCO_2 we present comparisons with global models using the output of two CO_2 assimilation systems (MACC version 14r2 and CarbonTracker version CT2013B). We show that overall there is reasonable consistency and agreement between all data sets (within ~1-2 ppm) but we also found significant differences depending on region and time period.

1. Introduction

Carbon dioxide (CO_2) is the most important human-emitted greenhouse gas responsible for global warming (IPCC, 2013). Despite its importance, our knowledge of the CO_2 sources and sinks has significant gaps and does not meet all needs for attribution, mitigation and the accurate prediction of future climate change (e.g., Stephens et al., 2007; Canadell et al., 2010; IPCC, 2013; Ciais et al., 2014). Despite efforts to reduce CO_2 emissions, atmospheric CO_2 continues to increase with currently approximately 2 ppm/year (e.g., Fig. 1 (satellite-derived column-averaged CO_2) and Le Quéré et al., 2015, based on Dlugokencky and Tans, 2015, NOAA/ESRL (near) surface CO_2 concentrations). The situation is similar for methane (CH_4; e.g., Dlugokencky et al., 2009; IPCC, 2013; Kirschke et al., 2013; Houweling et al., 2014; Alexe et al., 2015).

The goal of the GHG-CCI project (Buchwitz et al., 2015), which is one of several projects of ESA's Climate Change Initiative (CCI, Hollmann et al., 2013), is to generate global satellite-derived atmospheric CO_2 and CH_4 data sets with as high as possible new information content on regional CO_2 and CH_4 sources and sinks, i.e., surface fluxes, to be extracted, for example, via inverse modeling (e.g., Reuter et al., 2014a; Alexe et al., 2015). GHG-CCI generates data sets of the Essential Climate Variable (ECV) Greenhouse Gases (GHG) as required by the GCOS (Global Climate Observing System) defined as follows (GCOS, 2011): "Product Number A.8.1: Retrievals of greenhouse gases, such as CO_2 and CH_4, of sufficient quality to estimate regional sources and sinks".

Currently multi-year radiance measurements from two satellite instruments are used in GHG-CCI to retrieve information on atmospheric CO_2 and CH_4 with high near-surface-sensitivity: SCIAMACHY on ENVISAT (2002 - April 2012) (Burrows et al., 1995; Bovensmann et al., 1999) and TANSO-FTS on-board GOSAT (launched in 2009) (Kuze et al., 2009, 2014). Both instruments perform (or have performed) nadir observations in the near-infrared/short-wave-infrared (NIR/SWIR) spectral region covering the relevant absorption bands of CO_2, CH_4 and molecular oxygen (O_2). The latter is used to obtain the “dry-air column” needed to compute GHG column-averaged dry-air mole fractions, i.e., XCO_2 (in ppm) and XCH_4 (in ppb) from the retrieved GHG vertical columns (e.g., Buchwitz et al., 2005) and/or to obtain information on atmospheric scatterers, e.g., on aerosols and thin cirrus clouds. These two instruments are the two main sensors used within GHG-CCI but in the future other sensors with similar radiance observations may be added, e.g., NASA’s successfully launched OCO-2 mission for XCO_2 (Crisp et al., 2004; Bösch et al., 2011; Zhang et al., 2016) and ESA’s Sentinel-5-Precursor mission for XCH_4 (Veefkind et al., 2012; Butz et al., 2012).

During recent years significant progress has been made towards achieving the demanding satellite XCO_2 and XCH_4 requirements. Prior to the GHG-CCI project initial XCO_2 retrievals were available from SCIAMACHY (e.g., Buchwitz et al., 2005, 2007; Schneising et al., 2008, 2009) but only first preliminary GOSAT retrievals. Progress has been made in terms of improved data quality, time coverage and interpretation of satellite XCO_2 data products (using GHG-CCI and other products generated in Japan (e.g., Yoshida et al., 2013, Oshchepkov et al., 2011, 2013) and in the USA (e.g., O’Dell et al., 2012; Crisp et al., 2012)) to enhance our knowledge on the various sources and sinks of these gases (e.g., Basu et al., 2013; Maksyutov et al., 2013; Saeki et al., 2013; Chevallier et al., 2014; Takagi et al., 2014; Reuter et al., 2014a, 2014b; Houweling et al., 2015; Alexe et al., 2015).

For example, focusing on hemispheric data and on carbon-climate feedbacks, Schneising et al., 2014a, used SCIAMACHY XCO_2 retrievals to study aspects related to the terrestrial carbon sink by looking at co-variations of XCO_2 growth rates and seasonal cycle amplitudes with near-surface temperature. They found XCO_2 growth rate changes of 1.25+/-0.32 ppm/year/K (approximately 2.7+/-0.7

GtC/year/K; indicating less carbon uptake in warmer years consistent with a positive carbon-climate feedback) for the Northern Hemisphere in good agreement with CarbonTracker. The CO_2 seasonal cycle, which is driven primarily by terrestrial CO_2 uptake and release processes, has also been studied in several other publications (e.g., Reuter et al., 2013; Buchwitz et al., 2015; Lindqvist et al., 2015). Guerlet et al., 2013, analyzed GOSAT XCO_2 retrievals focusing on the Northern Hemisphere. They identified reduced carbon uptake in the summer of 2010 and found that this is most likely due to the heat wave in Eurasia driving biospheric fluxes and fire emissions. Using a joint inversion of GOSAT and surface data, they estimated an integrated biospheric and fire emission anomaly in April–September 2010 of 0.89±0.20 PgC over Eurasia. Basu et al., 2014, studied seasonal variations of CO_2 fluxes during 2009-2011 over Tropical Asia using GOSAT, CONTRAIL and IASI data. They found an enhanced source for 2010 and concluded that this is likely due to the biosphere response to above-average temperatures in 2010 and unlikely due to biomass burning emissions. Parazoo et al., 2013, used GOSAT XCO_2 and solar induced chlorophyll fluorescence (SIF) retrievals to better understand the carbon balance of southern Amazonia. Ross et al., 2013, used GOSAT data to obtain information on wildfire CH_4:CO_2 emission ratios. For flux inversions not only the retrieved greenhouse gas values are relevant but also their error statistics, in particular the reported uncertainties. Chevallier and O'Dell, 2013, analyzed this aspect in the context of CO_2 flux inversions using GOSAT XCO_2 retrievals. Detmers et al., 2015, analyzed GOSAT XCO_2 to detect and quantify anomalously large climate-related carbon uptake in Australia during the time period end of 2010 to early 2012. Furthermore, a number of publications focused on improving retrieval algorithms including data processing and comparisons with ground-based observations and global models (e.g. Heymann et al., 2012a, 2012b) or on applying existing algorithms to other sensors (e.g., Heymann et al., 2015). Satellite XCO_2 retrievals are also used, for example by the European Centre for Medium-Range Weather Forecasts (ECMWF), to characterize atmospheric CO_2 at large and synoptic scales and for CO_2 forecasting (Massart et al., 2016). Last but not least and despite the fact that none of the existing satellite missions has been optimized to obtain information on anthropogenic CO_2 emissions (in contrast to other proposed future missions, in particular CarbonSat (Bovensmann et al., 2010; Velazco et al., 2011; Buchwitz et al., 2013)) this important aspect has been addressed in several recent publications using existing satellite XCO_2 products (Kort et al., 2012; Schneising et al., 2013, Reuter et al., 2014b).

Nevertheless, not all carbon-related problems which have been addressed can be answered with confidence due to potential issues with the satellite retrievals (in particular remaining biases) and/or transport modelling (e.g., Stephens et al., 2007) as needed to interpret the satellite products (e.g., Chevallier et al., 2010; Deng et al., 2014). An example is the recent effort to quantify European biospheric terrestrial CO_2 fluxes. Basu et al., 2013, presented first CO_2 surface flux inverse modeling results from GOSAT XCO_2 retrievals for various regions including Europe. For Europe their results imply that Europe is a much stronger carbon sink than current knowledge suggests. Chevallier et al., 2014a, used an ensemble of inversion methods and GOSAT XCO_2 retrievals to also derive regional (sub-continental) CO_2 surface fluxes. They also found a significantly larger European carbon sink. They conclude that the derived sink is unrealistically large and they argue that this may be due to modelling issues related to long-range transport modelling and/or biases of the satellite retrievals. In particular they argue that errors of the satellite data outside of Europe may adversely influence the European results. To further investigate this European carbon sink issue in detail, Reuter et al., 2014a, used an ensemble of SCIAMACHY and GOSAT XCO_2 data products and an inversion method which is not, or at least significantly less, sensitive to the potential issues discussed in Chevallier et al., 2014a. For example, Reuter et al., 2014a, only used satellite XCO_2 retrievals over Europe to rule out that non-European satellite data adversely influence the results for the European carbon sink and they also only used short-term (days) transport modelling for satellite data interpretation to minimize potential long-range transport errors. Reuter et al., 2014a, also performed several sensitivity tests to investigate the robustness of their results and to establish a reliable error budget. Based on an extensive analysis they conclude: “We show that the satellite-derived European terrestrial carbon sink is indeed much larger (1.02 +/- 0.30 GtC/year in 2010) than previously expected”. The value they derived is larger compared to earlier inversion estimates using in-situ observations of 0.47 +/- 0.50 (“LSCE-39-insitu inversion”) or 0.42 +/- 0.25 (“UoE-insitu”) GtC/year for 2010 (Chevallier et al., 2014a), or 0.40 +/- 0.42 GtC/year for 2001-2004 (Peylin et al, 2013), which is reported in the recent

IPCC report (IPCC, 2013). The disagreement with bottom-up estimates is even larger and significant: Schulze et al., 2009, report 0.235 +/- 0.05 GtC/year between 2000 and 2005. These findings of Reuter et al., 2014a, stimulated additional research using satellite and non-satellite CO_2 observations (e.g., Feng et al., 2016, and discussion in Houweling et al., 2015) but consensus has not yet been achieved, e.g., Feng et al., 2016, finally conclude: "…we cannot prove or disprove that European ecosystems are taking up a larger-than-expected amount of CO_2". Recently, some new research results have been obtained by assimilating new Siberian CO_2 observations in CarbonTracker (Kim et al., 2016). They report a European sink strength of 0.75±0.63 GtC/year for 2008-2009, which temporally overlaps with the range reported by Reuter et al., 2014a, and is significantly larger compared to their reference inversions without these new Siberian observations. On the other hand, based on simultaneous CO_2 and CH_4 flux inversions using GOSAT-retrieved ratios of total column CH_4 and CO_2 for 2009 and 2010, Pandey et al., 2016, obtain European terrestrial CO_2 fluxes close to zero, in contrast to the results discussed above. Apparently, more research is needed to answer this important European carbon sink question with confidence.

For satellite XCH_4 retrievals and the interpretation of these data sets the situation is similar as for XCO_2. SCIAMACHY data have already been extensively used to improve our knowledge on atmospheric methane and regional methane emissions prior to the start of the GHG-CCI project (e.g., Buchwitz et al., 2005; Frankenberg et al., 2005; Schneising et al., 2009; Bergamaschi et al., 2007, 2009; Bloom et al., 2010). A more recent research focus has been to investigate the unexpected renewed atmospheric methane increase since 2007 using ground-based and/or satellite data (e.g., Rigby et al., 2008; Dlugokencky et al., 2009; Bergamaschi et al., 2009, 2013; Schneising et al., 2011; Frankenberg et al., 2011; Sussmann et al., 2012; Crevoisier et al., 2013; Houweling et al., 2014; Nisbet et al., 2014; Schaefer et al., 2016). Methane emission estimates have been obtained from GOSAT as discussed in a number of recent publications (e.g., Fraser et al., 2013, 2014, Monteil et al., 2013, Cressot et al., 2014, Alexe et al., 2015; Turner et al., 2015, 2016). In these studies often CH_4 retrievals from several satellites have been used (as well as other data, in particular NOAA data), e.g., Monteil et al., 2013, and Alexe et al., 2015, used SCIAMACHY and GOSAT retrievals, Cressot el al., 2014, used

GOSAT, SCIAMACHY and IASI, and Wecht et al., 2014, and Worden et al., 2015, used GOSAT and TES satellite retrievals. Several publications focused on relatively localized methane sources, e.g., in the United States: For example, Schneising et al., 2014, analyzed SCIAMACHY data over major US “fracking” regions and quantified anthropogenic methane emissions and leakage rates and also others used SCIAMACHY data over the US to identify and quantify localized methane emission sources (Kort et al., 2014; Wecht et al., 2014). The SCIAMACHY XCH_4 retrievals have also been used to compare with and to improve chemistry-climate models (Shindell et al., 2014, Hayman et al., 2014).

Despite this quite large number of publications it is clear that still much more has to be learned about the various (and changing) sources and sinks of CO_2 and CH_4. It is obvious that the more accurate and precise the observations are and the longer and denser the observational time series is, the larger their information content. Within the GHG-CCI project a continuous algorithm improvement, re-processing and data product analysis cycle is carried out every year with the goal to deliver each year an improved data set of satellite-derived atmospheric CO_2 and CH_4 information. The latest data set is called CRDP3. This data set is presented in the following (Sect. 2) including an initial quality assessment by comparison with ground-based observations (Sect. 3) and model comparisons (Sects. 4 and 5) focusing on CO_2. A summary and conclusions are given in Sect. 6.

2. Overview data set CRDP3

The GHG-CCI latest data set called Climate Research Data Package No. 3 (CRDP3) consists of several satellite-derived atmospheric CO_2 and CH_4 data products. These data products are classified as (i) GHG-CCI project core products, generated with so-called ECV Core Algorithms (ECAs), and (ii) additional products, generated with so-called Additional Constraints Algorithms (ACAs). The ECA products are XCO_2 and XCH_4 (see Tabs. 1 and 2) retrieved from satellite nadir mode radiance spectra in the near-infrared / shortwave-infrared (NIR/SWIR) spectral region using appropriate retrieval algorithms. These retrieval algorithms are all based on modelling the observed radiance spectra using a radiative transfer model and corresponding parameters (e.g., vertical profiles of atmospheric CO_2,

CH_4, temperature, aerosols, etc.) coupled to an inversion method to iteratively optimize selected parameters until the modeled radiance matches the observed radiance spectrum. All retrieval algorithms are based on Optimal Estimation / Bayesian Inference theory (see Rodgers, 2000, for the general theory and Reuter et al., 2010, for a typical example) with the exception of the WFMD algorithms (see Tabs. 1 and 2), which are based on a least-squares fitting combined with a very fast look-up-table scheme (e.g., Buchwitz et al., 2000; Schneising et al., 2011). The algorithms are also using post-processing steps including bias correction and quality filtering and/or assigning a quality flag to each single retrieval (ground pixel) (see information on retrieval Algorithm Theoretical Baseline Documents (ATBDs) given below).

Table 1: Overview GHG-CCI individual ECV Core Algorithms (ECAs) as used for XCO_2 retrieval and the generation of the corresponding data product. See main text for a description of baseline and alternative products.

GHG-CCI ECV Core Algorithms (ECAs) for XCO_2 retrieval			
Algorithm ID (Version)	**Sensor**	**Algorithm Institute**	**Comment (Algorithm reference)**
CO2_SCI_BESD (v02.01.01)	SCIAMACHY/ ENVISAT	BESD IUP, Univ. Bremen, Germany	SCIAMACHY XCO_2 baseline product Coverage: global (land), 1.2003-3.2012 (Reuter et al., 2011)
CO2_SCI_WFMD (v3.9)	-“-	WFM-DOAS IUP, Univ. Bremen, Germany	SCIAMACHY XCO_2 alternative product Coverage: global (land), 10.2002-4.2012 (Schneising et al., 2011)
CO2_GOS_OCFP (v6.0)	TANSO/GOSAT	UoL-FP University of Leicester (UoL), UK	GOSAT XCO_2 baseline product Coverage: global, 4.2009-12.2014 (Cogan et al., 2012)
CO2_GOS_SRFP (v2.3.7)	-“-	RemoTeC SRON (Utrecht, Netherlands) & KIT (Karlsruhe, Germany)	GOSAT XCO_2 alternative product Coverage: global, 6.2009-12.2014 (Butz et al., 2011)

Table 2: As Tab. 1 but for the GHG-CCI individual XCH_4 retrieval algorithms and corresponding data products.

GHG-CCI ECV Core Algorithms (ECAs) for XCH_4 retrieval			
Algorithm ID (Version)	**Sensor**	**Algorithm Institute**	**Comment (Algorithm reference)**
CH4_SCI_WFMD (v3.9)	SCIAMACHY/ ENVISAT	WFM-DOAS IUP, Univ. Bremen, Germany	SCIAMACHY XCH_4 proxy product (baseline not yet decided) Coverage: global, 10.2002-12.2011 (Schneising et al., 2011)
CH4_SCI_IMAP (v7.1)	-"-	IMAP SRON (Utrecht, Netherlands) & JPL (Padadena, CA, USA)	SCIAMACHY XCH_4 proxy product (baseline not yet decided) Coverage: global (land), 1.2003-4.2012 (Frankenberg et al., 2011)
CH4_GOS_OCPR (v6.0)	TANSO/GOSAT	UoL-PR University of Leicester (UoL), UK	GOSAT XCH_4 proxy baseline product Coverage: global, 4.2009-12.2014 (Parker et al., 2011)
CH4_GOS_SRPR (v2.3.7)	-"-	RemoTeC SRON (Utrecht, Netherlands) & KIT (Karlsruhe, Germany)	GOSAT XCH_4 proxy alternative product Coverage: global, 6.2009-12.2014 (Butz et al., 2010)
CH4_GOS_SRFP (v2.3.7)	-"-	RemoTeC SRON (Utrecht, Netherlands) & KIT (Karlsruhe, Germany)	GOSAT XCH_4 full physics baseline product Coverage: global, 6.2009-12.2014 (Butz et al., 2011)
CH4_GOS_OCFP (v1.0)	-"-	UoL-PR University of Leicester (UoL), UK	GOSAT XCH_4 full physics alternative product Coverage: global, 4.2009-12.2014 (Parker et al., 2011)

The exploited NIR/SWIR spectral regions contain relevant CO_2, CH_4 and (depending on algorithm/product) molecular oxygen (O_2) absorption lines. O_2 is used to get information on the light path and on the dry-air column needed to convert the GHG vertical columns into mole fractions (number density mixing ratio). For sufficiently cloud-free day-side observations these spectra are typically dominated by surface-reflected solar radiation and are therefore sensitive to near-surface greenhouse gas concentration variations.

Currently, the corresponding GHG-CCI ECA products are derived from SCIAMACHY/ENVISAT and TANSO/GOSAT. In this publication we focus on the GHG-CCI CRDP3 ECA products. An overview on the additional GHG-CCI ACA products is given in Buchwitz et al., 2015, and details are given on the GHG-CCI website (http://www.esa-ghg-cci.org/), in particular in the corresponding ACA product tables as given on the GHG-CCI main data products website (http://www.esa-ghg-cci.org/sites/default/files/documents/public/documents/GHG-CCI_DATA.html). In short, ACA products are not (or typically not) sensitive to near-surface GHG variations but to variations in upper atmospheric layers, i.e., layers above the planetary boundary layer. They therefore provide complementary additional information (compared to ECAs) on atmospheric CO_2 and CH_4. ACA products are mid/upper tropospheric CO_2 and CH_4 mixing ratios from IASI (Crevoisier et al., 2009a, 2009b, 2013), upper tropospheric / stratospheric vertical CH_4 profiles from MIPAS (Laeng et al., 2015), stratospheric CH_4 and CO_2 profiles from SCIAMACHY solar occultation observations (Noël et al., 2012, 2016) and stratospheric CO_2 profiles from ACE-FTS (Foucher et al., 2009).

An overview about the GHG-CCI ECAs and corresponding data products is given in Tab. 1 for XCO_2 and in Tab. 2 for XCH_4. As can be seen, there are two algorithms for each data product. For example, there are two algorithms for XCO_2 from SCIAMACHY and two algorithms for XCO_2 from GOSAT, resulting in four XCO_2 products generated independently with different algorithms. We encourage users of our data products to take advantage of this ensemble of products which can even be extended using additional (i.e., non-GHG-CCI) products generated elsewhere, most notably in Japan (NIES products (Yoshida et al., 2013; Oshchepkov et al., 2011, 2013) and in the USA (NASA ACOS product

(O'Dell et al., 2012; Crisp et al., 2012)). The main reason for this recommendation is that even small (and typically difficult to characterize) systematic errors in the XCO_2 products can lead to quite large errors when using XCO_2 to get information on CO_2 surface fluxes (emission or uptake). This is because the CO_2 background concentration is quite high and even large sources and sinks typically results in only small XCO_2 variations (see, e.g., Reuter et al., 2014a). Using an ensemble of products generated with independent algorithms enables one to determine the robustness of the source/sink findings with respect to algorithmic choices which have to be made when implementing a retrieval algorithm and also permits one to assign more realistic error bars to quantitative source/sink results (see, for example, Reuter et al., 2014a, using an ensemble of XCO_2 data products to obtain information on the strength of the European carbon sink).

However, we acknowledge that this is a major effort which cannot be undertaken by all users, e.g., due to time, financial or other constraints. For these users we aim at giving recommendations on which product to use if they can or want to use only one (or a few) products. We do this by identifying so-called baseline (or recommended) products (see also Buchwitz et al., 2015, and Dils et al., 2014, for our initial "Round Robin" attempt to identify "best" algorithms and corresponding data products). As can be seen from Tabs. 1 and 2, we have identified baseline algorithms/products for all products except for SCIAMACHY XCH_4 (as both products still suffer from degraded quality as discussed below). Note that a baseline product is not necessarily significantly better than the corresponding alternative product because, as one may expect, different algorithms have different strengths and weaknesses. Often we found that data products differ (e.g., at the different individual validation sites) but it is not clear which one is better (e.g., if the overall agreement with the validation network is on average equivalently good). Therefore, for products where this is the case, the baseline product is for some products simply the product which has been agreed upon between the different data providing institutions. Note that the definition of "better" also depends on the application. For example, for SCIAMACHY XCO_2, the BESD product has been declared as baseline product and the WFMD product as alternative product because BESD has typically lower systematic errors / biases, and better precision, i.e., less random errors (as confirmed by the results shown in Sect. 3.1) but much less data (approx. 50% as also shown in Sect. 3.1) compared to the WFMD product. For some applications with relevant requirements on spatio-temporal coverage, the WFMD product may therefore be the better suited or even the only choice provided the biases are small enough for the target application. Within the GHG-CCI project quality assessment is an ongoing effort with one of the goals to confirm or change the classification of algorithms/products as "baseline" or "alternative", depending on future algorithm improvements and corresponding future data quality.

Note that two additional XCO_2 and XCH_4 products are available from the GHG-CCI website not listed in Tabs. 1 and 2. These are the Ensemble Median Algorithm (EMMA) XCO_2 (Reuter et al., 2013) and XCH_4 products. These products are also Level 2 products (i.e., non-gridded individual ground pixel swath products) as the other products listed in Tabs. 1 and 2 but they have been generated by merging individual products from SCIAMACHY and GOSAT. They are not further discussed here (for details see Reuter et al., 2013, and Buchwitz et al., 2016).

As can be seen from Tab. 2, the number of XCH_4 algorithms/products is even larger than for XCO_2. The reason is that there are two types of XCH_4 algorithms for the GOSAT products, the so-called (light path) "proxy" (PR) algorithms and the "full-physics" (FP) algorithms (see Schepers et al., 2012, Buchwitz et al., 2015, Parker et al., 2015, and references given therein for details). In short, XCH_4 PR algorithms convert retrieved CH_4 columns into XCH_4 by using dry-air columns obtained from simultaneously retrieved CO_2 column in combination with modelled CO_2 column to correct for CO_2 column variations (the PR algorithm require that atmospheric CH_4 columns typically vary more than CO_2 columns (in relative, i.e., percentage, terms)). The advantage of the PR method is that systematic column retrieval errors (e.g., light path errors due to unaccounted scattering by aerosols and clouds but also some instrument errors) cancel to some extent when the ratio of the retrieved CH_4 and CO_2 columns is computed. The disadvantage is that this method needs sufficiently accurate CO_2 model simulations to correct for CO_2 variations. The FP method, which does not have this disadvantage, aims at considering aerosol and cirrus effects explicitly by considering (as good as possible) the "full physics" of the atmospheric radiative transfer. This means that FP methods aim at solving a much more challenging radiative transfer and inversion problem and, therefore, they do not have to rely on accurate CO_2 modelling. This shows that both methods have different strengths and weaknesses. As a consequence the resulting data products have different characteristics (typically PR products contain much more data points compared to FP products, see Sect. 3.2). Because these two type of methane algorithms/products are significantly different they are classified separately as baseline or alternative as shown in Tab. 2.

Despite the fact that all algorithms are based on similar principles (namely on optimizing radiative transfer model and other parameters until a "good" match between the measured and modelled radiances has been obtained), they differ in many details. It is out of the scope of this manuscript to explain each algorithm in detail. Instead we refer to the documentation as given on the GHG-CCI website, in particular to the Algorithm Theoretical Baseline Documents (ATBDs) (see links given in the product tables of the GHG-CCI main data products website (http://www.esa-ghg-cci.org/sites/default/files/documents/public/documents/GHG-CCI_DATA.html)).

Figure 1 shows time series of northern hemispheric XCO_2 as obtained from all four GHG-CCI XCO_2 retrieval algorithms (see Tab. 1). As can be seen, all XCO_2 products clearly show an approximately 2 ppm/year CO_2 increase (due to anthropogenic CO_2 emissions) and the atmospheric CO_2 seasonal cycle (primarily due to regular uptake and release of CO_2 by the terrestrial biosphere). The SCIAMACHY products cover (essentially) the entire ENVISAT time period from end of 2002 (WFMD product) or beginning of 2003 (BESD product) to April 2012. The GOSAT CRDP3 products cover the time period mid 2009 to end of 2014. As can be seen, the agreement between the different time series is within about 1-2 ppm. Note that perfect agreement is not to be expected, e.g., due to differences in spatio-temporal sampling and vertical sensitivity (see the following sections for quantitative assessments). To obtain quantitative estimates of the characteristics of the various data products in terms of random and systematic errors and long-term stability one has to compare the individual products with appropriate high-quality reference data (see Sect. 3) and one also has to compare spatial pattern (Sect. 4). In Sect. 3 we present comparisons of the satellite products with ground-based observations at selected locations and in Sect. 4 we present comparison with global models. Note that we also aim at model independent quantitative comparisons of the global satellite data via the Ensemble Median Algorithm EMMA (Reuter et al., 2013). For the latest EMMA assessment results (not shown here) see Buchwitz et al., 2016.

Figure 2 shows time series of northern hemispheric XCH_4. As can be seen, the agreement among the various products is less good (in relative terms) compared to XCO_2 in particular for the two SCIAMACHY XCH_4 products which also deviate significantly from the GOSAT XCH_4 products in particular for 2010 and later years. This is potentially due to SCIAMACHY detector issues whose impact on the data quality is still large but hopefully can be (further) mitigated in future versions of the SCIAMACHY products. The seasonality of the GOSAT XCH_4 OCFP product, which is a new product from Univ. Leicester, deviates somewhat from the other products. Also this aspect needs further investigation.

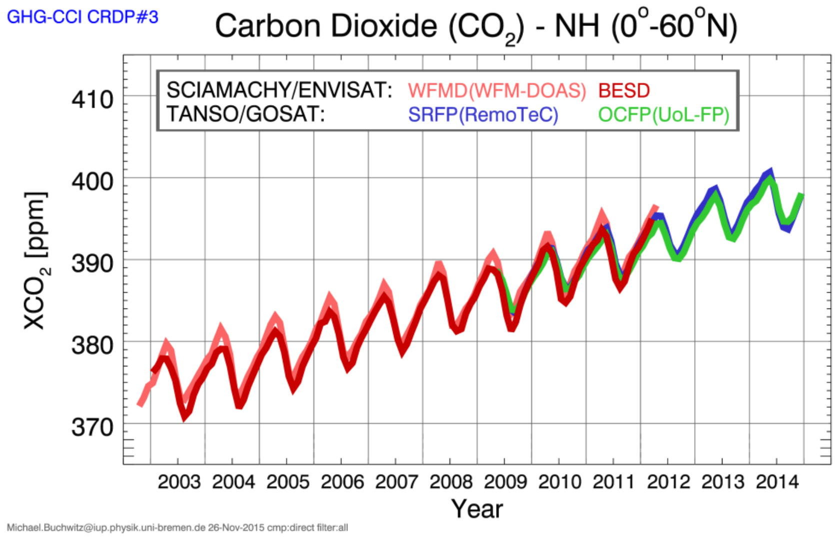

Figure 1: Timeseries of northern hemispheric XCO_2 of the four GHG-CCI CRDP3 XCO_2 data products (CO2_SCI_WFMD (light red), CO2_SCI_BESD (red), CO2_GOS_SRFP (blue) and CO2_GOS_OCFP (green)) obtained by averaging all satellite retrievals north of the equator up to 60°N for each month.

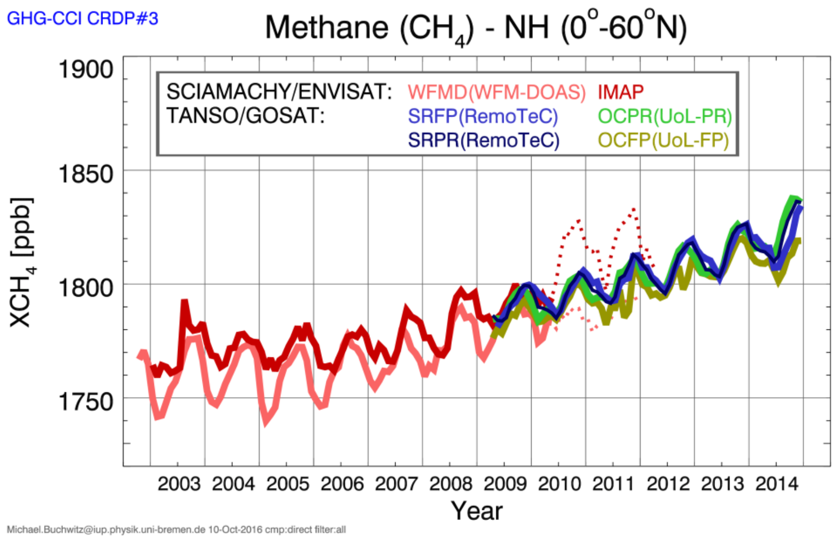

Figure 2: Timeseries of northern hemispheric XCH_4 of the six GHG-CCI CRDP3 XCH_4 data products (see inset) obtained by averaging all satellite retrievals north of the equator up to 60°N for each month. Note that the SCIAMACHY products after approx. mid 2010 (see dotted lines) suffer from currently still unresolved issues probably related to detector degradation.

In the following section a comparison of these XCO_2 and XCH_4 products with ground-based reference observations is presented which has been carried out to obtain initial quantitative information on the data quality. Note that a more detailed comparison with ground-based data is presented in Dils et al., 2016.

3. Comparisons with ground-based observations

The ground-based Total Carbon Column Observing Network (TCCON) has been designed for validation of satellite XCO_2 and/or XCH_4 retrievals (Wunch et al., 2011a, 2011b) and TCCON data have been used extensively also in the past for comparison of GHG-CCI data products (e.g., Dils et al., 2014, Buchwitz et al., 2015). TCCON is a network of ground-based Fourier Transform Spectrometers recording direct solar spectra in the near-infrared spectral region. From these spectra, accurate and precise column-averaged abundance of CO_2, CH_4 and other atmospheric data products are retrieved. The TCCON XCO_2 and XCH_4 data products version GGG2014 as used for this study (Wunch et al., 2015) have been downloaded from the TCCON data archive (http://tccon.ornl.gov).

Within GHG-CCI we use several somewhat different methods for satellite – TCCON comparison (see Buchwitz et al., 2016) including methods developed and applied independently by each data provider to his/her product. Two methods are applied to all CRDP3 XCO_2 and XCH_4 products, the method developed by the GHG-CCI validation team (Dils et al. 2016) and a somewhat simplified approach developed and used primarily for Quality Control / Quality Assurance (QC/QA) purposes. Overall it has been found that all validation methods result in similar conclusions concerning the overall data quality of the CRDP3 ECA products, which demonstrates the robustness of the findings (Buchwitz et al., 2016). In the following we present the QC/QA approach and its results.

For QC/QA of the CRDP3 ECA products we have used version GGG2014 (Wunch et al., 2015) XCO_2 and XCH_4 TCCON data products from six TCCON sites, two in the USA, two in Europe and two in

Australia (see Tab. 3). For each ECA product and each of the selected TCCON sites we have performed detailed comparisons of individual (but also averaged) satellite soundings (ground pixels) using a co-location criterion of 2 hours temporally and 4^ox4^o latitude/longitude spatially. To minimize the impact of different *a priori* information used for the retrievals, common CO_2 and CH_4 profiles have been used for comparison using TCCON *a priori* profiles as common profiles for the comparisons (see also Dils et al., 2014, using the same approach).

Table 3: TCCON sites and corresponding data coverage as used for comparison with the satellite XCO_2 and XCH_4 data products. The "Time coverage" corresponds to the time coverage of the data products at the time of data access (6-Oct-2015, except Bremen and Bialystok: 20-Nov-2015).

TCCON validation sites					
Location (TCCON data product reference)	**Site ID**	**Latitude [deg]**	**Longitude [deg]**	**Altitude [km]**	**Time coverage MM/YYYY-MM/YYYY**
ParkFalls, USA (Wennberg et al., 2014a)	PAR	45.945	-90.273	0.442	06/2004 - 12/2014
Lamont, USA (Wennberg et al., 2014b)	LAM	36.604	-97.486	0.320	07/2008 - 12/2014
Bremen, Germany (Notholt et al., 2014)	BRE	53.104	8.850	0.027	01/2007 - 10/2014
Bialystock, Poland (Deutscher et al., 2014)	BIA	53.231	23.025	0.183	03/2009 - 10/2014
Darwin, Australia (Griffith et al., 2014a)	DAR	-12.425	130.891	0.030	08/2005 - 09/2014
Wollongong, Australia (Griffith et al., 2014b)	WOL	-34.406	150.879	0.030	06/2008 - 09/2014

When interpreting satellite-TCCON differences one also has to consider the uncertainty of the TCCON data products. TCCON uncertainties are reported in the TCCON data product files for each individual observation and these uncertainties have been used, e.g., to avoid using TCCON data with large reported errors. However, what is also needed, in particular to compute systematic satellite-TCCON differences across several sites (see, e.g., summary values for regional and seasonal biases in Tabs. 4 and 5) is an estimate of the TCCON site-to-site bias and/or an estimate of the TCCON uncertainty after averaging many TCCON retrievals. Site-to-site biases for TCCON products are reported in Wunch et al., 2010. As shown in Wunch et al., 2010, the uncertainty of the TCCON data products is typically 0.4 ppm for XCO_2 (1-sigma) and 4 ppb (1-sigma) for XCH_4 (see also the discussion of this and corresponding implications for interpreting satellite - TCCON comparisons as reported in Dils et al., 2014, and Buchwitz et al., 2015). Due to these uncertainties / potential errors of the TCCON data (but also for other reasons, e.g., non-perfect spatio-temporal co-location) the estimated systematic and random errors of the satellite retrievals as reported here have to be interpreted as upper limit estimates (because we assume here that the TCCON site-to-site bias is zero), i.e., the satellite data product errors are likely smaller than reported here, at least at the TCCON sites. On the other hand the TCCON network is quite sparse and does not cover all geophysical conditions. For example, for the XCO_2 products it has been identified that differences between satellite products located far away from TCCON sites may differ by somewhat larger amounts than the TCCON validation suggests (e.g., Reuter et al., 2013). Because of these potential overestimation (neglection of TCCON site-to-site bias) / underestimation (TCCON does not capture all situation) issues we interpret the differences to TCCON reported here as a reasonable estimate of the real error (which can be compared with the user requirements) without taking the uncertainty of the TCCON retrievals explicitly into account, i.e., we assume that underestimation and overestimation effects cancels to a large extent (at least on average).

As shown in the following two sub-sections, we compare the achieved performance with the required performance as specified by GCOS (GCOS, 2011) and with the typically more demanding and more detailed requirements as specified in the GHG-CCI User Requirements Document (URD, Chevallier et al., 2014b). Note that GCOS is not explicitly specifying requirements for XCO_2 and XCH_4 but for „Tropospheric CO_2 column“ and „Tropospheric CH_4 column“ in mole fraction (mixing ratio) units (e.g., ppm for CO_2). In this manuscript we interpret the GCOS requirements as listed in GCOS, 2011, as requirements for XCO_2 and XCH_4.

Table 4: Comparison results for product CO2_SCI_BESD with TCCON XCO_2 at six TCCON sites. In the top part of the table results are listed per TCCON site. Reported in column “Bias” are the regional and seasonal biases (see main text for details), the “Scatter”, which is the standard deviation of satellite-TCCON difference (based on the individual satellite soundings, i.e., ground pixel) and “RepUncert” (reported uncertainty), which is the mean value of the reported uncertainty as given in the satellite product files for each single sounding. “UncRat” is the uncertainty ratio, which is the ratio of RepUnc and Scatter. Values close to unity indicate that the reported uncertainty is (on average) reliable. “Trend” characterises the long-term stability as obtained by fitting a straight line to the satellite minus TCCON differences covering the entire time series. The listed trend error is the 3-sigma uncertainty of the slope of the fitted line. Nobs are the number of individual satellite soundings compared to TCCON. In the bottom part of the table summary values are listed for each parameter (the sum or the mean and/or the standard deviation). See main text for details.

Site ID	**Bias [ppm]**		**Scatter [ppm]**	**RepUnc [ppm] (UncRat [-])**	**Trend (Stability) [ppm/year]**	**Nobs [-]**
	Regional	**Seasonal**				
PAR	-0.2	0.8	2.0	2.1 (1.0)	0.14 +/- 0.04	2931
LAM	-0.3	0.7	1.7	1.9 (1.1)	-0.01 +/- 0.05	12003
BRE	-0.3	0.8	1.8	2.5 (1.4)	-0.13 +/- 0.13	1036
BIA	-0.2	1.0	2.0	1.9 (1.0)	0.03 +/- 0.17	1124
DAR	-0.5	0.9	1.8	1.7 (0.9)	-0.02 +/- 0.04	7323
WOL	0.5	0.6	2.2	2.1 (0.9)	-0.07 +/- 0.11	2389
Summary:						
Sum						26806
Mean	-0.2	0.8	1.9	2.0 (1.1)	-0.01 +/- 0.09	
StdDev	0.4					

Table 5: As Tab. 4 but for product CH4_SCI_WFMD.

Site ID	Bias [ppb]		Scatter [ppb]	RepUnc [ppb] (UncRat [-])	Trend (Stability) [ppb/year]	Nobs [-]
	Regional	Seasonal				
PAR	5.0	19.6	78.2	67.3 (0.9)	0.77 +/- 0.84	11079
LAM	4.5	10.5	75.1	84.1 (1.1)	0.23 +/- 2.00	18725
BRE	2.9	18.4	91.8	85.8 (0.9)	-1.86 +/- 4.80	1512
BIA	6.2	18.9	88.8	84.2 (0.9)	6.88 +/- 7.62	2230
DAR	-18.1	17.2	67.9	82.7 (1.2)	-1.87 +/- 1.38	10580
WOL	-16.2	16.4	88.0	82.0 (0.9)	7.73 +/- 5.34	2832
Summary:						
Sum						46958
Mean	-2.6	16.8	81.6	81.0 (1.0)	1.98 +/- 3.66	
StdDev	11.3					

3.1 XCO_2 comparisons with TCCON

Figure 3 shows as an example a comparison of the CO2_SCI_BESD product with TCCON XCO_2 retrievals at Lamont, Oklahoma, USA. As can be seen, several figures of merit are listed in Fig. 3. They have been defined and computed for quantitative characterization of systematic and random errors of the satellite products and to determine if there are linear trends in the satellite-TCCON differences, i.e., to assess the long-term stability of the satellite products. We also aim at validating the reported uncertainty, which is given in the GHG-CCI data products for each single retrieval (i.e., for each individual ground pixel). This has been done by computing the ratio of the mean value of the reported uncertainty to the standard deviation of the difference to TCCON. Figures such as Fig. 3 have been generated for all ECA XCO_2 products and all selected TCCON sites (not shown). The most important figures of merit for product CO2_SCI_BESD at all six TCCON sites are presented in Tab.

4. Table 4 also lists summary results (obtained by computing the sum, the mean and/or the standard deviation of the results obtained at the individual TCCON sites). The summary results for all four XCO_2 products are listed in Tab. 6.

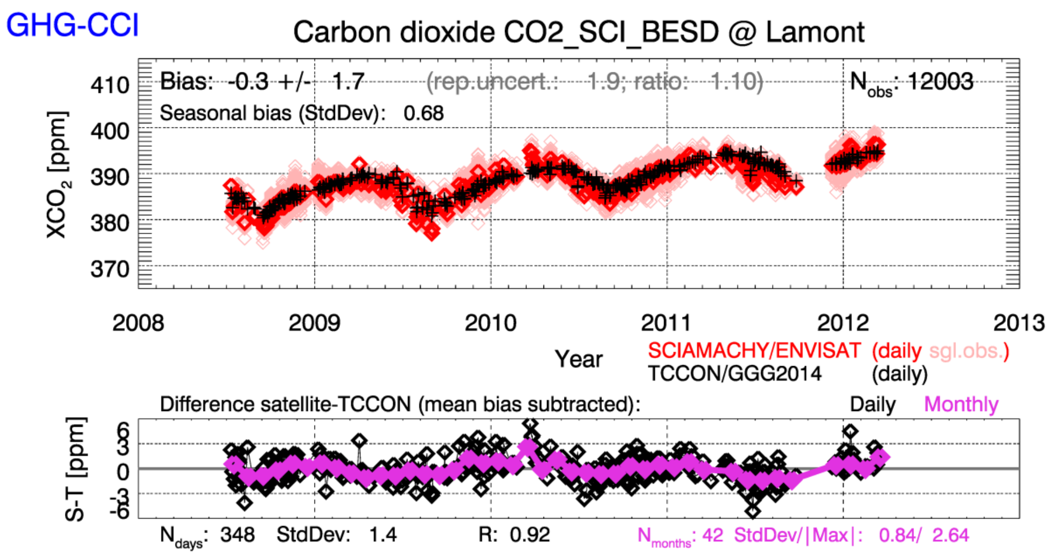

Figure 3: Comparison of product CO2_SCI_BESD with TCCON XCO_2 at TCCON site Lamont, Oklahoma, USA. Top: Satellite XCO_2 in light red for the individual soundings, i.e., single observations ("slg. obs.") and red for daily averages (co-location criterion: +/- 4 degrees, +/- 2 hours). TCCON XCO_2 is shown in black. Listed are several figures of merit: "Bias" (mean +/- standard deviation of the difference of the individual satellite retrievals and TCCON), "Seasonal bias" (standard deviation of differences for 3-month time periods), "Nobs" (number of individual satellite retrievals) and in grey the mean value of the reported uncertainty of the individual XCO_2 retrievals ("rep. uncert.") and the "ratio" of the reported uncertainty and the standard deviation of the difference to TCCON. Bottom: XCO_2 difference at daily (black) and monthly (pink) resolution. The listed key figures of merit are also shown in Tab. 4 along with the corresponding values obtained at other TCCON sites.

Table 6: Overall TCCON comparison results for the GHG-CCI XCO_2 products. The results for product CO2_SCI_BESD have been obtained from Tab. 4 (the corresponding tables for the other three products are not shown here). “Systematic error” lists the regional and seasonal biases and, in brackets, a combined values ($bias_{tot}$ (see Eq. (1)). “Uncertainty” is the mean value of the reported uncertainty and uncertainty ratio “UncRat” (in brackets) is defined as for Tab. 4. Also listed is the “Trend” (with 3-sigma uncertainty), “Offset” (the mean difference relative to all TCCON sites) and the number of satellite soundings (“Nobs”) compared to TCCON. At the bottom the corresponding requirements are listed based on GCOS, 2011, and on the GHG-CCI User Requirements Document (URD) (specified as Goal (G), Breakthrough (B) and Threshold (T)) (Chevallier et al., 2014b). Note that the GCOS requirements are target (maximum) requirements, whereas the URD threshold requirements are minimum requirements. The URD requirement for the systematic error is therefore much more demanding than the GCOS requirement but the stability requirements are identical. Note that the uncertainty of the TCCON reference data used to obtain the estimates listed here is about 0.4 ppm (1-sigma).

Product	**Systematic error [ppm]** Regional, seasonal (combined)	**Uncertainty (Random error) [ppm]** (UncRat)	**Trend (Stability) [ppm/year]**	**Offset [ppm]**	**Nobs [-]**
CO2_SCI_BESD	0.4, 0.8 (0.9)	1.9 (1.1)	-0.01 +/- 0.09	-0.2	26806
CO2_SCI_WFMD	0.6, 1.1 (1.3)	3.0 (1.1)	0.01 +/- 0.10	0.6	50087
CO2_GOS_OCFP	0.3, 0.5 (0.6)	1.7 (1.4)	-0.11 +/- 0.14	0.1	6139
CO2_GOS_SRFP	0.6, 0.5 (0.8)	1.9 (1.0)	-0.08 +/- 0.11	0.1	6795
Required G / B / T	< 1 < 0.2 / 0.3 / 0.5	- < 1 / 3 / 8	< 0.2 < 0.2 / 0.3 / 0.5	GCOS (2011) GHG-CCI URD (Chevallier et al., 2014b)	

As can be seen from Tab. 6, column “Systematic error”, the estimated regional bias of product CO2_SCI_BESD is 0.4 ppm and the estimated seasonal bias is 0.8 ppm. The regional bias has been estimated as standard deviation of the biases obtained at the individual TCCON sites (“station-to-station bias”) (see Tab. 4 for CO2_SCI_BESD). The seasonal bias is the mean value (over all TCCON sites) of the standard deviation of 3-monthly biases as obtained at the individual TCCON sites (see Dils et al., 2014, for a similar estimation of biases). The method of computing standard deviations neglects a possible overall offset relative to TCCON (listed separately in Tab. 6) but this is in line with the GHG-CCI User Requirements Document (URD, Chevallier et al., 2014b) which explains that spatio-temporal variations of biases are critical but overall (constant) offsets can be dealt with when using the satellite data products for inverse modelling (in other words “relative accuracy” is more important than “absolute accuracy”; note that in this manuscript the terms “accuracy”, “systematic error” and “bias” have the same meaning). Furthermore, a combined systematic error, $bias_{tot}$, is listed in column “Systematic error” in brackets, which has been computed from the regional and seasonal biases as follows:

$$bias_{tot} = \sqrt{bias_{reg}^2 + bias_{seas}^2} \qquad \text{Eq. (1)}$$

As can be seen from Tab. 6, the biases of the other products are quite similar. All values are below 1 ppm except for product CO2_SCI_WFMD, where the total bias is 1.25 ppm. Tab. 6 also lists the required performance. As can be seen, all products (with the exception of CO2_SCI_WFMD, which has the advantage of providing the largest number of data points) meet the GCOS systematic error requirement (of better than 1 ppm) but not the much more demanding requirement as listed in the GHG-CCI URD (better than 0.5 ppm). However, as already mentioned above, one also has to consider the uncertainty of the TCCON retrievals (see also Buchwitz et al., 2015, for a discussion of this aspect). The systematic and random errors of single TCCON data are typically 0.4 ppm for XCO_2 (1-sigma) and 4 ppb (1-sigma) for XCH_4 (see Notholt et al., 2012, based on Wunch et al., 2010).

Assuming an overall TCCON bias uncertainty of 0.4 ppm for XCO_2 (see also Kulawik et al., 2016) and adding this (in a root-sum-square manner (e.g., Eq. (1)) to the 0.5 ppm URD requirement yields 0.64 ppm, i.e., a number somewhat larger than the overall bias for product CO2_GOS_OCFP (0.58 ppm). It is therefore possible that product CO2_GOS_OCFP even meets the demanding GHG-CCI URD threshold systematic error requirement of better than 0.5 ppm.

Table 6 also lists mean values of the reported uncertainty (essentially the random error component of the single ground pixel satellite retrievals) and the "uncertainty ratio" ("UncRat", in brackets), i.e., the ratio of reported uncertainty and standard deviation of the difference to TCCON. For the CO2_SCI_BESD product the reported uncertainty is 1.9 ppm (on average) and the uncertainty ratio is 1.1 providing confidence that the reported uncertainty is realistic (at least on average). This is also true for the other products with the exception of CO2_GOS_OCFP which appears to overestimate the uncertainty by about 40% on average, i.e., the reported uncertainty is quite conservative. As can also be seen, all products clearly meet the GHG-CCI URD breakthrough requirement of better than 3 ppm or are very close to meeting it (for product CO2_SCI_WFMD the estimated precision is 3.0 ppm).

Table 6 also lists the linear trend and its uncertainty, which has been determined by fitting a straight line to the individual satellite minus TCCON differences (after removal of a possible seasonal cycle obtained by fitting a linear combination of harmonics (sine and cosine functions) to the data). The trend uncertainty as given here is the 3-sigma uncertainty of the estimated trend. Assuming that only trends which are larger than their uncertainty are significant, one can see that none of the trends is significant. This indicates very good long-term stability (or, more precisely, the absence of a linear drift) of all satellite XCO_2 products (note that even the goal requirement of better than 0.2 ppm/year is met for all products).

3.2 XCH_4 comparisons with TCCON

Similar comparisons as presented in the previous sub-section have also been performed for the XCH_4 ECA products. Detailed example results for product CH4_SCI_WFMD are shown in Fig. 4 and Tab. 5. The most relevant figures of merit, defined as for XCO_2 (see previous section), are summarized along with the results for the other products in Tab. 7.

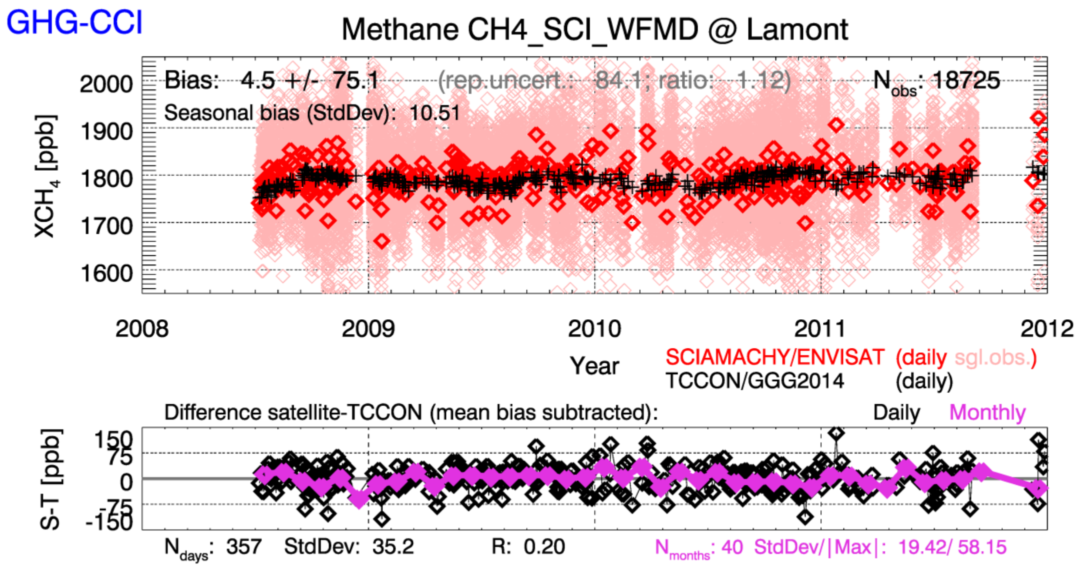

Figure 4: As Fig. 3 but for product CH4_SCI_WFMD.

As can be seen from Tab. 7, the (relative) biases are around 20 ppb for the SCIAMACHY products, which is worse than the required performance of better than 10 ppb. A much better performance in the range 6-7 ppb has been achieved for the GOSAT products (which, however, contain significantly less observations). The GOSAT products meet the GCOS and GHG-CCI URD systematic error (“accuracy”) requirements.

As can also be seen from Tab. 7, the GOSAT products also meet the GHG-CCI breakthrough requirement for random errors (better than 17 ppb) in contrast to the SCIAMACHY products which do not meet the threshold requirement. However one has to point out that the first years of SCIAMACHY, where the data quality is much higher, is under-represented here as no TCCON observations are available during the first nearly two years of the ENVISAT mission (see Tab. 3).

Table 7: As Tab. 6 but for the GHG-CCI XCH_4 products. Note that the uncertainty of the TCCON reference data used to obtain the estimates listed here is about 4 ppb (1-sigma).

Product	**Systematic error [ppb]** Regional, seasonal (combined)	**Uncertainty (Random error) [ppb]** (UncRat)	**Trend (Stability) [ppb/year]**	**Offset [ppb]**	**Nobs [-]**
CH4_SCI_WFMD	11.3, 16.8 (20.3)	81.6 (1.0)	2.0 +/- 4.3	-2.6	46958
CH4_SCI_IMAP	14.8, 14.4 (20.7)	48.3 (1.3)	4.5 +/- 2.8	-13.2	64841
CH4_GOS_OCPR	4.6, 3.4 (5.7)	11.9 (1.0)	0.0 +/- 1.1	6.5	14639
CH4_GOS_SRPR	3.4, 5.1 (6.1)	12.8 (0.9)	-0.9 +/- 1.0	-2.6	13502
CH4_GOS_SRFP	4.7, 5.1 (6.9)	12.6 (1.0)	-1.0 +/- 1.3	-1.4	6819
CH4_GOS_OCFP	4.1, 5.7 (7.0)	13.4 (0.7)	-0.4 +/- 1.2	0.7	5913
Required **G / B / T**	< 10 < 1 / 5 / 10	- < 9 / 17 / 34	< 2 < 1 / 5 / 10	GCOS (2011) GHG-CCI URD (Chevallier et al., 2014b)	

Table 7 also shows that the GOSAT products are very stable meeting the GCOS and (typically) even the GHG-CCI URD goal requirement. The SCIAMACHY products do not meet the GCOS stability requirement but apparently meet the GHG-CCI breakthrough requirement (of less than 5 ppb/year), at least concerning linear long-term drifts. However we also looked at shorter-term drifts of biases and identified issues in particular for the year 2010 and later years due to remaining issues from detector degradation (see Fig. 2).

4. XCO_2 comparisons with global models

In the previous section we have presented validation results at selected TCCON sites. We have also performed detailed validation at a much larger number of TCCON sites as shown in Dils et al., 2016. Nevertheless, the number of ground-based validation sites is limited and large parts of the Earth are not covered (e.g., Africa, South America and large parts of Asia). Therefore, we present in this section detailed comparisons with global data sets (for recent comparisons with global models addressing different aspects see also Lindqvist et al., 2015, Parker et al., 2015, Kulawik et al., 2016). Here we use the output of the two global CO_2 assimilation systems (“models”) MACC (Chevallier et al., 2015), version 14r2, and CarbonTracker (Peters et al., 2007), version CT2013B. Note that comparisons with global models as well as CO_2 flux inversion results using CRDP3 XCO_2 (and XCH_4) are also presented and discussed in Chevallier et al., 2016.

The European MACC (Monitoring of Atmospheric Composition Change) / CAMS (Copernicus Atmospheric Monitoring System) project global atmospheric CO_2 reanalysis data product, version v14r2, has been obtained from the MACC/CAMS website (http://macc.copernicus-atmosphere.eu/catalogue/ -> http://apps.ecmwf.int/datasets/data/macc-ghg-inversions/, access: 23-Feb-2016). The MACC Bayesian inversion method (e.g., Chevallier et al., 2015, and references given therein) is formulated in a variational way in order to estimate CO_2 surface fluxes at relatively high resolution over the globe. Fluxes and mole fractions are linked in the system by the global atmospheric transport model of the Laboratoire de Météorologie Dynamique (LMDZ) with 39 layers in the vertical and with the same horizontal resolution than the inverted fluxes. LMDZ is nudged to ECMWF-analysed winds for flux inversion. The MACC inversion product also contains the 4-D CO_2 field that is associated to the inverted surface fluxes through the LMDZ transport model. These 4-D fields have been used for this study. Satellite XCO_2 observations have not been assimilated in MACCv14r2.

The CarbonTracker atmospheric CO_2 data product, version CT2013B, has been obtained from the NOAA/ESRL CarbonTracker website (http://www.esrl.noaa.gov/gmd/ccgg/carbontracker/, access: 3-Dec-2015) on which a detailed description of this version and how it has been generated is given. In short, CarbonTracker, developed by the National Oceanic and Atmospheric Administration (NOAA) Earth System Research Laboratory (ESRL), is an atmospheric CO_2 inverse modeling system that estimates optimized weekly surface CO_2 flux using the Ensemble Kalman Filter (EnKF) technique. Since the initial CarbonTracker release (Peters et al., 2007), a series of improvements have been made with subsequent releases. These include increasing the sites from which CO_2 data are assimilated, increasing the resolution of atmospheric transport, improving the simulation of atmospheric convection in the underlying transport model (TM5), and the use of multiple first-guess flux models to estimate dependence on priors. These improvements are documented at http://carbontracker.noaa.gov. CT2013B is a revision to the previous release (CT2013) and has the same time span, 2000-2012. For CT2013B the atmospheric transport model has been significantly improved. CT2013B assimilates CO_2 observations which are part of ESRL's new ObsPack data delivery system (http://www.esrl.noaa.gov/gmd/ccgg/obspack/, Masarie et al., 2014). Satellite XCO_2 observations have not been assimilated in CT2013B.

In the following we show comparisons of three GHG-CCI XCO_2 products with these two models in order to find out if it is possible to identify which of the model data sets compares best with the satellite data. The comparison has been done for the years 2010 and 2011 as these are the two years where the SCIAMACHY and GOSAT time series overlap.

Figure 5a shows comparisons of the GHG-CCI satellite-derived XCO_2 data products BESD, SRFP and OCFP with the MACC and CarbonTracker (CT) model data sets for the time period June-August (JJA) 2010 at a resolution of 2^ox2^o. The model data have been sampled according to the time and location of the (individual) satellite retrievals and the satellite averaging kernels have been applied to the model data to consider the altitude sensitivity of the satellite retrievals when computing XCO_2

from the model CO_2 profiles (see Buchwitz et al., 2014). This has been done for each single satellite sounding (ground pixel) and afterwards the model data and the satellite data have been averaged (gridded 2^ox2^o) to obtain the maps shown in Fig. 5a.

The first row of Fig. 5a shows global maps of the three satellite data products. As can be seen, their spatial coverage differs. For example, the SCIAMACHY BESD data set is restricted to observations over land whereas the two GOSAT products also contain observations over oceans (corresponding to GOSAT sun-glint mode observations). As can also be seen, the spatial XCO_2 pattern over land show similarities but also differences. For example, all three products show elevated XCO_2 (red color) over similar parts of the western USA and Mexico, Amazonia and India and low XCO_2 over parts of eastern Russia but different patterns over Africa, in particular northern Africa. These differences could be a result of the different sampling (different spatio-temporal coverage) of the satellite data products within the JJA time period (due to differences of the SCIAMACHY and GOSAT overpass time and the different quality filtering procedures of the different retrieval algorithms).

To investigate the effect of spatio-temporal sampling one can compare the satellite retrievals with the model data sets. The middle row of Fig. 5a shows the MACC model sampled as the three satellite data products (e.g., the left panel in the middle row entitled MACC@CO2_SCI_BESD is the MACC model sampled as the BESD product). MACC sampled as the three satellite products (middle row) also shows elevated XCO_2 (red color) over similar parts of the western USA and Mexico, Amazonia and India in good to reasonable agreement with the satellite retrievals. Overall, all three MACC maps show similar XCO_2 pattern indicating that the pattern does not depend significantly on the sampling of the satellite data products. Over northern Africa MACC and OCFP show quite similar pattern whereas SRFP XCO_2 is significantly higher. There are nearly no BESD data over northern Africa as most of the BESD retrievals have been removed by the very strict BESD quality filter.

The bottom row of Fig. 5a shows CT sampled as the three satellite data products. Overall, there is good agreement between CT and MACC but there are also differences. For example, CT shows significantly lower XCO_2 over large parts of eastern Russia compared to MACC. The satellite products show XCO_2 values which are in between the values of MACC and CT but are significantly closer to MACC (see also Fig. 5b discussed below). This may indicate that over eastern Russia the CT XCO_2 is somewhat too low during summer (JJA season; note that we get similar comparison results also for JJA 2011 not shown here).

Figure 5b shows the differences between the models and the satellite data (first two rows) and the difference between the two models (bottom row). The bottom row shows that the largest difference between the two models is over large parts of eastern Russia with differences up to about +4 ppm (MACC higher than CT). For other regions the agreement is mostly in the range +/-2 ppm (green color). As can also be seen, the satellite data are in better agreement with MACC over eastern Russia.

To also consider the uncertainty of the satellite retrievals we have generated Fig. 5c. Our estimated uncertainties are shown in the bottom row of Fig. 5c. These uncertainties (unc_{tot}) have been computed as follows:

$$unc_{tot}(N) = \sqrt{bias_{tot}^2 + \frac{rnd^2}{N}} \qquad \text{Eq. (2)}$$

Here N are the number of satellite retrievals per (2°x2°) grid cell, $bias_{tot}$ is the systematic error component of the total uncertainty (see Eq. (1) and Tab. 6) and *rnd* is the random error component of the total uncertainty for single observations, which is assumed here to improve with $\sqrt{N}$ when N observations are averaged (see also Kulawik et al., 2016, and Sect. 5 for an assessment of how SCIAMACHY and GOSAT XCO_2 uncertainties depend on the number of observations added). *rnd* has been computed by averaging the reported uncertainties of the N XCO_2 retrievals located in each grid cell. Here the reported uncertainties of the CO2_GOS_OCFP product have been divided by 1.4 to compensate for the approximately 40% overestimation of the reported errors (see previous discussion of the results presented in Tab. 6). As can be seen from the bottom row of Fig. 5c, the uncertainty of the three satellite data products is typically around 1.2 ppm (standard deviation 0.5 ppm).

The first two rows displayed in Fig. 5c show the same model minus satellite differences as also shown in Fig. 5b but restricted to those (2^ox2^o) grid cells where the (absolute value of the) difference is larger than the uncertainty shown in the bottom row, i.e., the first two rows only show cells with likely "significant differences". As can be seen, OCFP shows hardly any significant differences at least for extended regions (of connected cells). An exception is the already discussed part of eastern Russia, where differences are significant for CT (for all three satellite products) but not for MACC. Over parts of Amazonia MACC XCO_2 is higher than BESD but this difference is much smaller for CT. Over parts of central Africa both models are higher than BESD. SRFP shows extended regions of differences over parts of northern Africa, Saudi Arabia and Iran (SRFP higher than the models as already mentioned when discussing Fig. 5a).

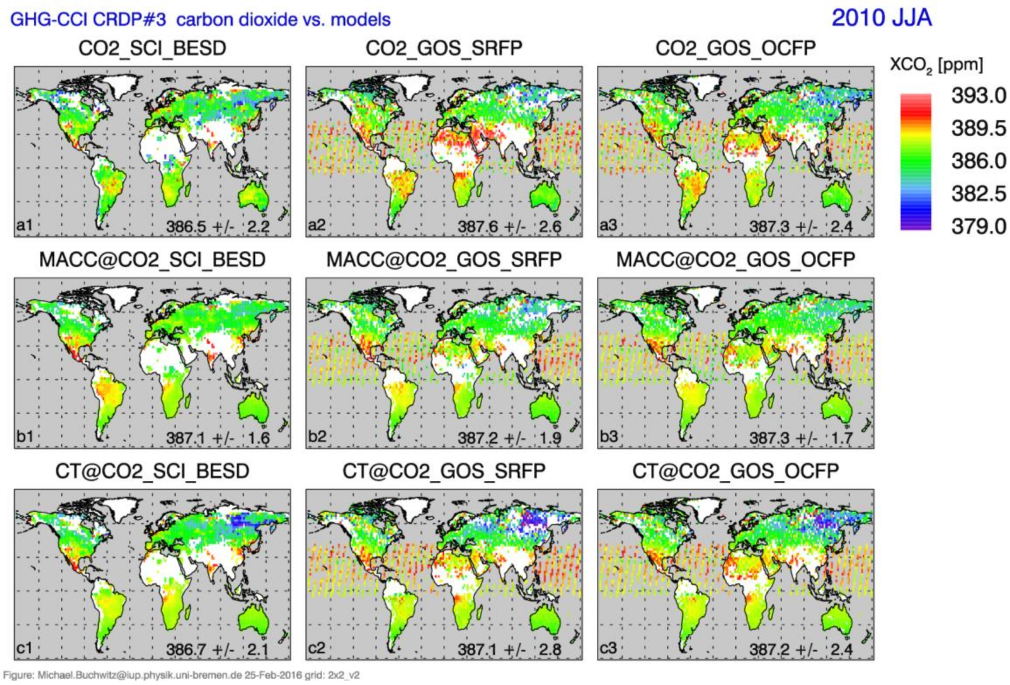

Figure 5a: Top: Satellite XCO_2 gridded 2^ox2^o for June-August 2010 for the three products BESD (left), SRFP (middle) and OCFP (right). Middle: MACC XCO_2 sampled as the three satellite products. Bottom: CarbonTracker sampled as the satellite products.

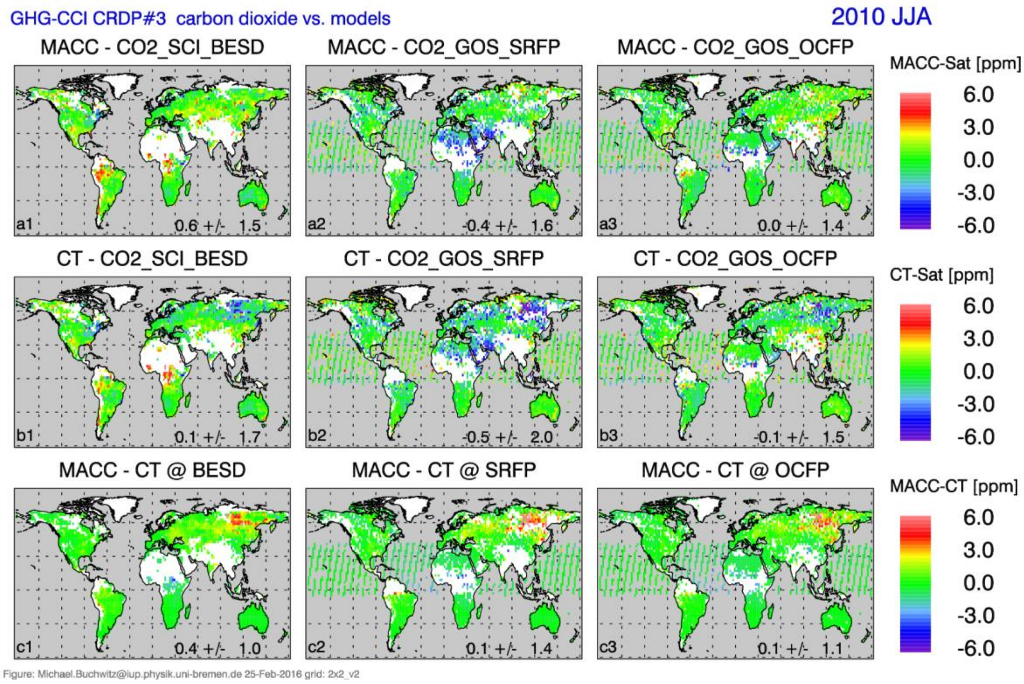

Figure 5b: As Fig. 5a but for the difference MACC-satellite (top), CarbonTracker-satellite (middle) and MACC-CarbonTracker (bottom) sampled according to the three satellite products BESD (left), SRFP (middle) and OCFP (right).

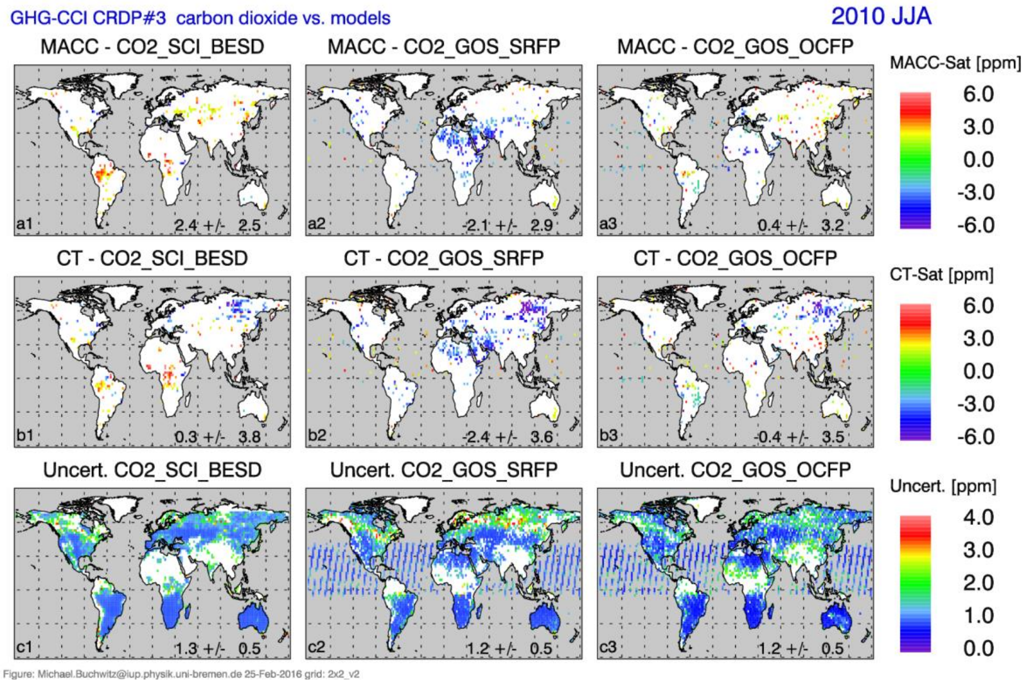

Figure 5c: As Fig. 5b but only for "significant" satellite-model differences (top and middle row) obtained by considering the uncertainty of the satellite retrievals (bottom). See main text for details.

Figures 6a – 6c show the same maps as Figs. 5a – 5c but for the time period September – November 2011. Here the models show differences in particular over parts of Amazonia, southern Africa and India (Figs. 6a) of about 2-3 ppm (Figs. 6b, bottom). The “significant differences” between the models and the satellite retrievals are shown in Figs. 6c (top row for MACC; middle row for CT). Over Amazonia and parts of southern Africa MACC is higher than BESD over large regions, whereas CT shows less differences to BESD over Amazonia and hardly any differences over southern Africa. For southern Africa the differences between the models and BESD are similar as for OCFP. Over Africa both models are lower compared to SRFP. Over India both models, MACC and CT, are lower than SRFP and OCFP.

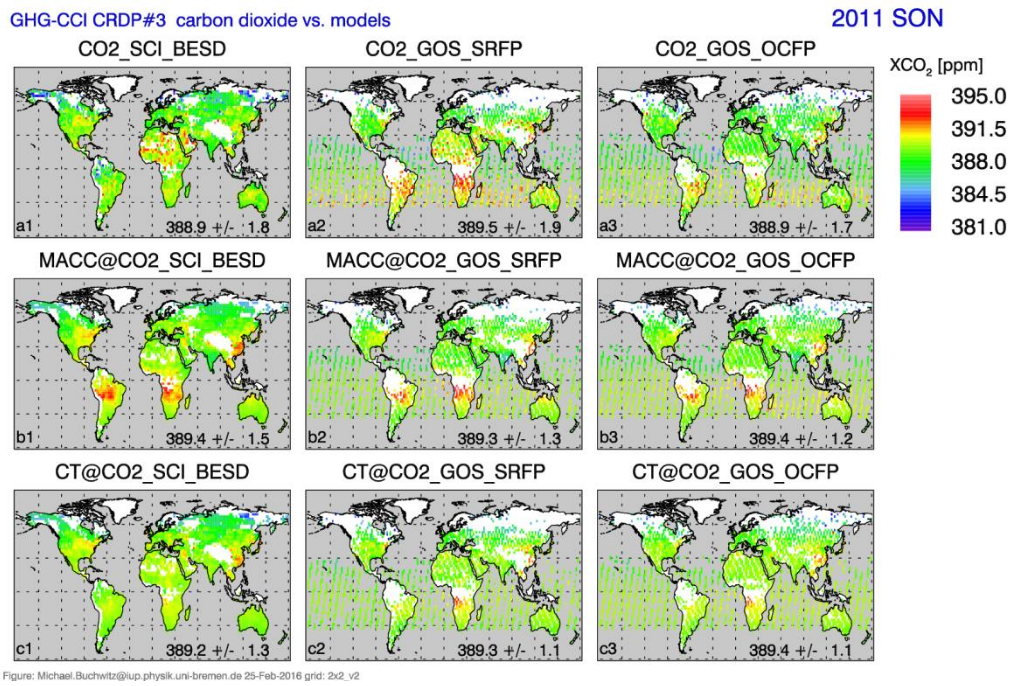

Figure 6a: As Fig. 5a but for September-November 2011.

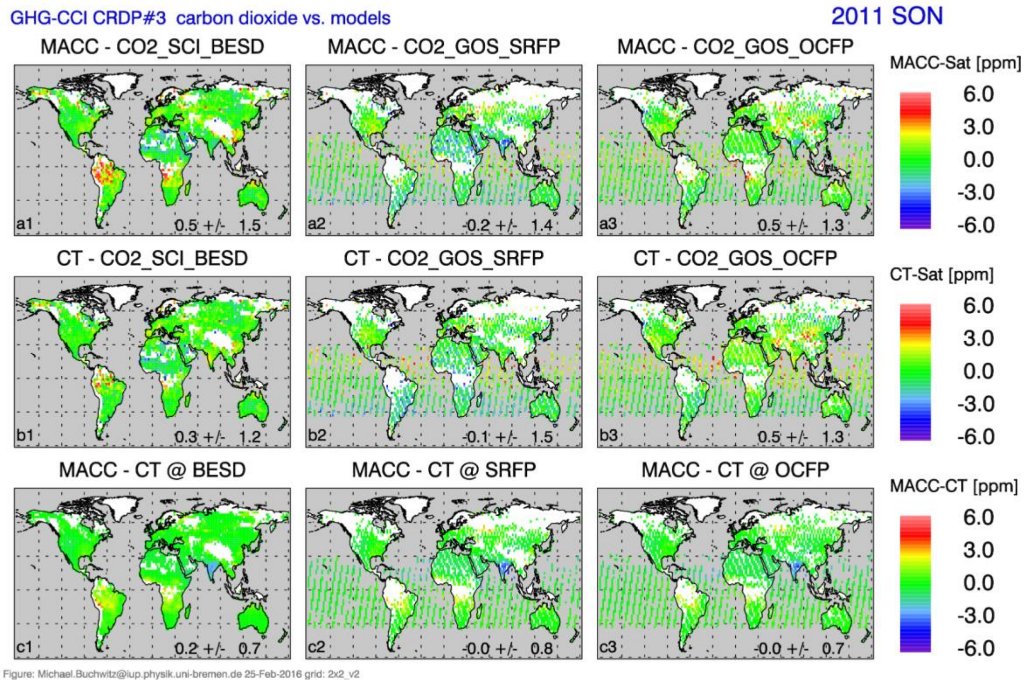

Figure 6b: As Fig. 5b but for September-November 2011.

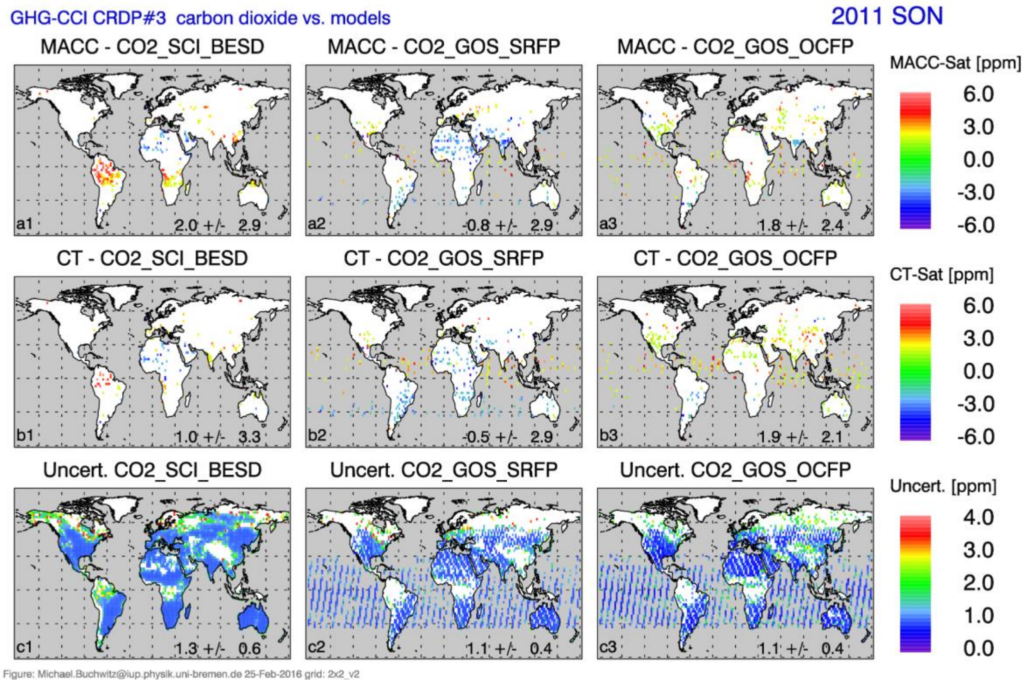

Figure 6c: As Fig. 5c but for September-November 2011.

To further investigate the agreements / disagreements between the XCO_2 data sets we also generated time series. Figures 7 – 11 show time series of the satellite and model data sets for some of the discussed regions but also for other regions. Figure 7 shows time series for the region southern Africa (SAF) based on monthly averages. The top left panel shows BESD XCO_2 (in red), MACC (black) and CT (grey) sampled as BESD. The panel on the right next to that panel shows the model – BESD differences as solid lines (in black for MACC and grey for CT) but also the estimated uncertainty (1-sigma) of the satellite data (red vertical bars, one for each month). As can be seen, both models are higher by about 0.6 ppm compared to BESD (top row), lower by about 0.7 ppm compared to SRFP (middle), whereas the average difference is close to zero for OCFP. The standard deviation of the monthly differences is 0.5 ppm for BESD for both models, for SRFP 0.3 ppm relative to MACC and 0.5 ppm relative to CT, and for OCFP 0.5 ppm relative to MACC and 0.6 ppm relative to CT. Note that typically the agreement between the models and the satellite retrievals is best where the number of satellite observations is highest (see N_{obs} bars in light red). Overall, OCFP shows the best agreement with the two models with most of the differences within 1 ppm.

Figs. 8 - 11 also show time series as Fig. 7 but for the regions northern Africa (NAF, Fig. 8). North America (NAM, Fig. 9), Europe (EUR, Fig. 10) and China (CHI, Fig. 11). For region NAF (Fig. 8), BESD and OCFP agree with the models within typically 1 ppm whereas SRFP has an apparent high bias of around 1.4 ppm. For region NAM (Fig. 9) the situation is similar for BESD and OCFP but the agreement is better for SRFP. For Europe (Fig. 10) the two models agree with each other but show typically a high bias compared to the satellite retrievals. For China (Fig. 11) the models typically agree with SRFP and OCFP within 1 ppm whereas the comparison with BESD shows somewhat larger differences for some months.

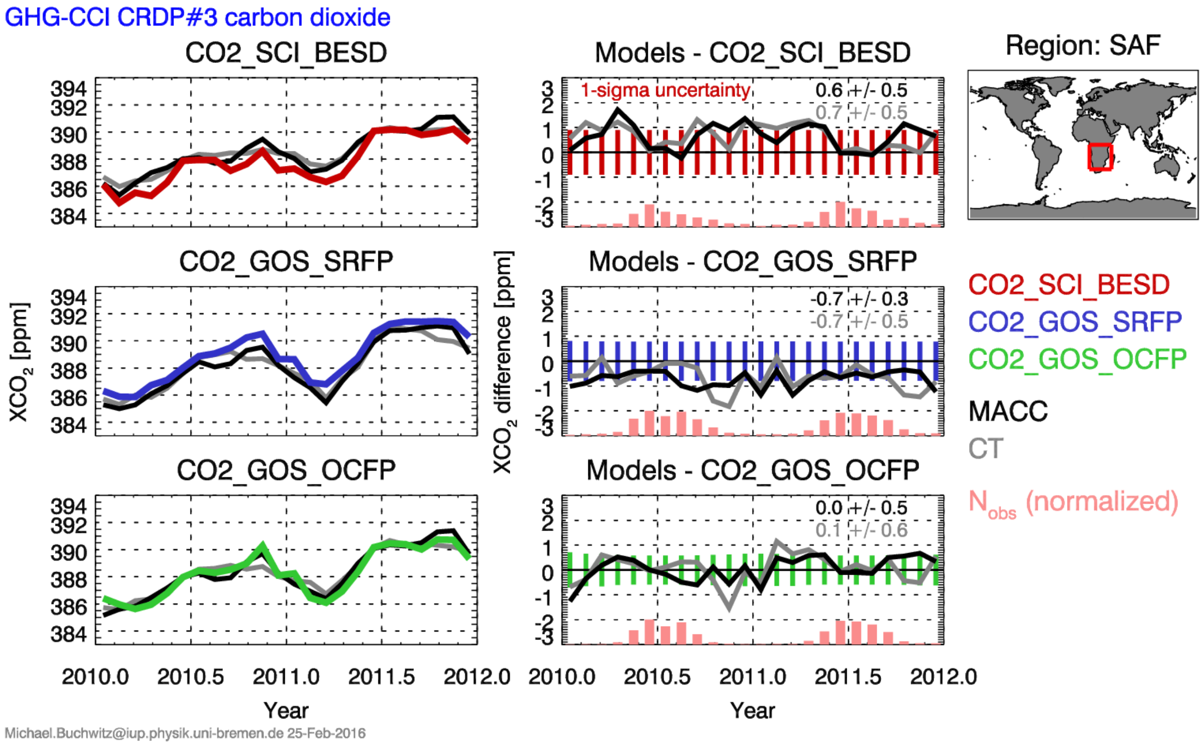

Figure 7: Timeseries of satellite and model XCO_2 for region Southern Africa (SAF; see map top right). Top left: Monthly XCO_2 BESD (red), MACC XCO_2 sampled as BESD (black) and CarbonTracker XCO_2 sampled as BESD (grey). Top middle: models – satellite for BESD: MACC-BESD (black) and CarbonTracker-BESD (grey). The red vertical bars indicate the estimated uncertainty of the satellite retrievals. In light red the number of satellite observations per month is shown (in arbitrary units). Middle: as top row but for SRFP (blue), Bottom: as top and middle row but for OCFP (green). Listed on top right in each panel on the right hand side is mean +/- standard deviation of the difference between the models and the satellite XCO_2.

Overall it can be concluded that the models agree with the satellite retrievals within typically 1-2 ppm but depending on region and time period differences can also be somewhat larger. As shown in Kulawik et al., 2016, MACC and CT fit TCCON typically quite well but TCCON stations are usually in place where there are surface air sample measurements to constrain the models (see also Parker et al., 2015). Differences may therefore be larger elsewhere. Nevertheless, we found that the two model data sets are very similar, in particular when averaged over large region (see regional timeseries).

However, we also identified significant differences between them. For example, CT shows significantly lower XCO_2 compared to MACC (approximately 4 ppm) over large parts of eastern Russia during summer 2010 (JJA season) (also during JJA 2011, but this has not been shown here). Over parts of Amazonia and southern Africa during autumn 2011 (SON season) MACC is about 2 ppm higher than CT and over India MACC is about 2-3 ppm lower (also for SON 2010, not shown here). We also identified significant differences between the satellite data products, e.g., a high or a low bias of SRFP compared to the other two satellite products BESD and OCFP depending on region and time period.

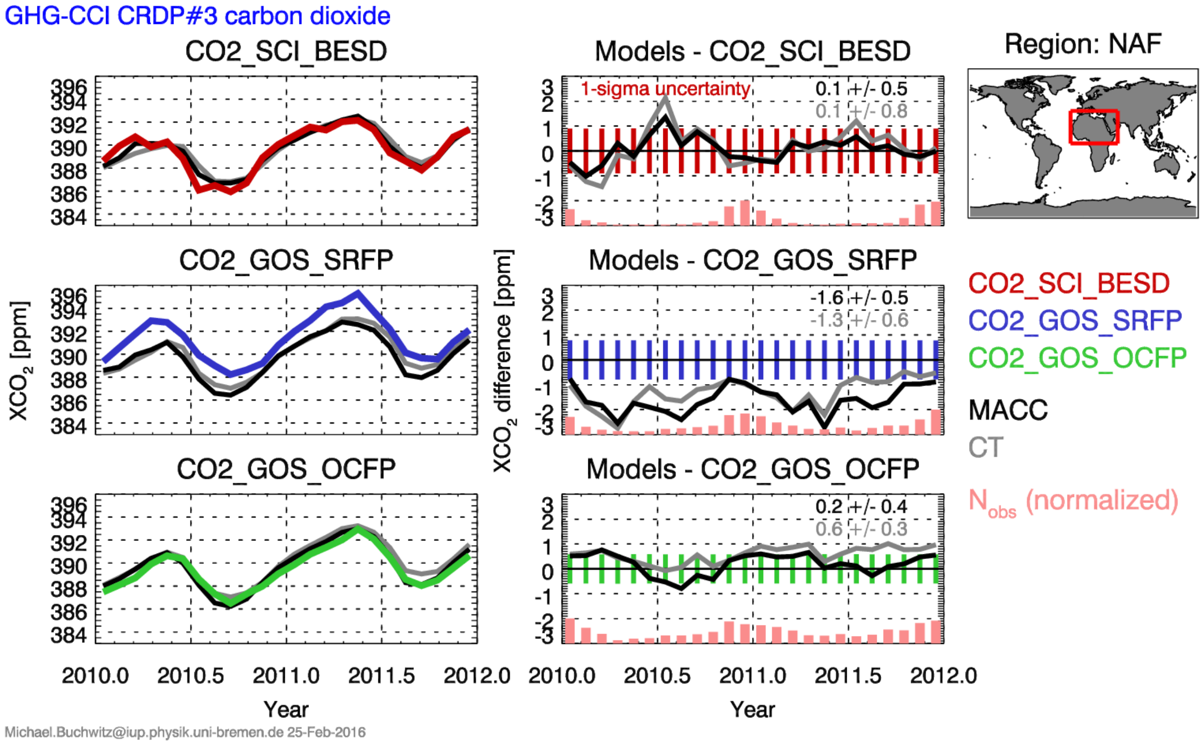

Figure 8: As Fig. 7 but for region Northern Africa (NAF).

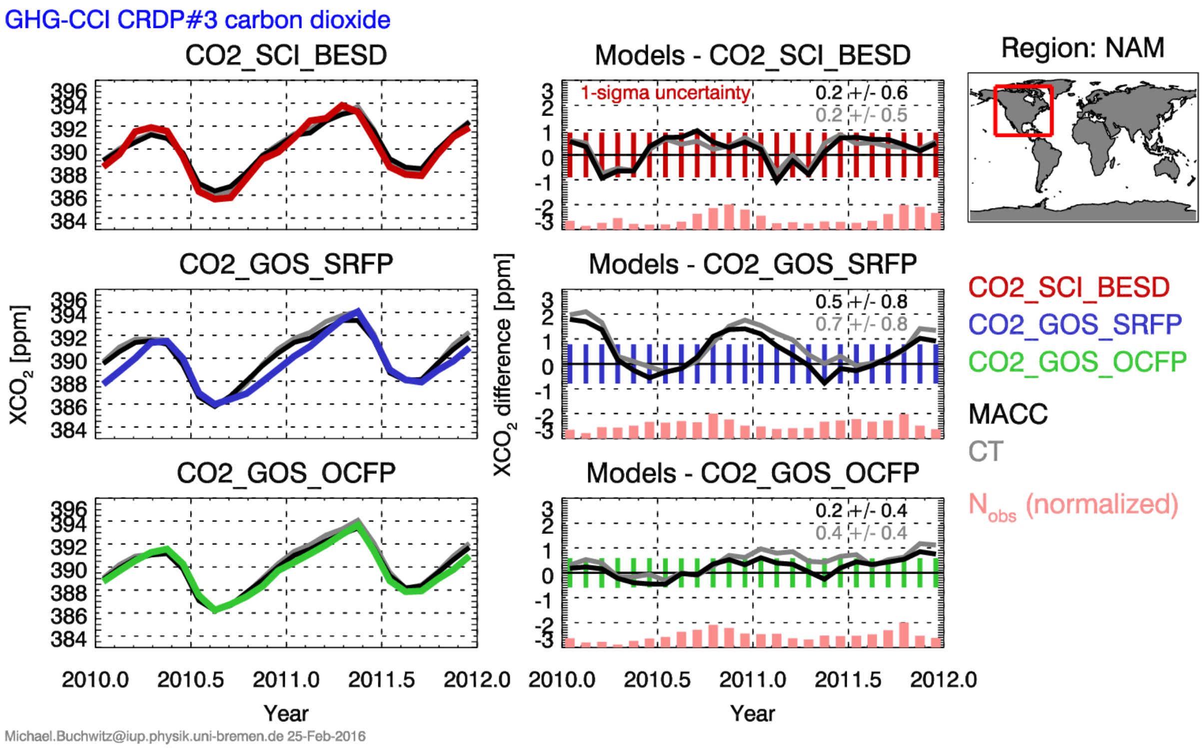

Figure 9: As Fig. 7 but for region North America (NAM).

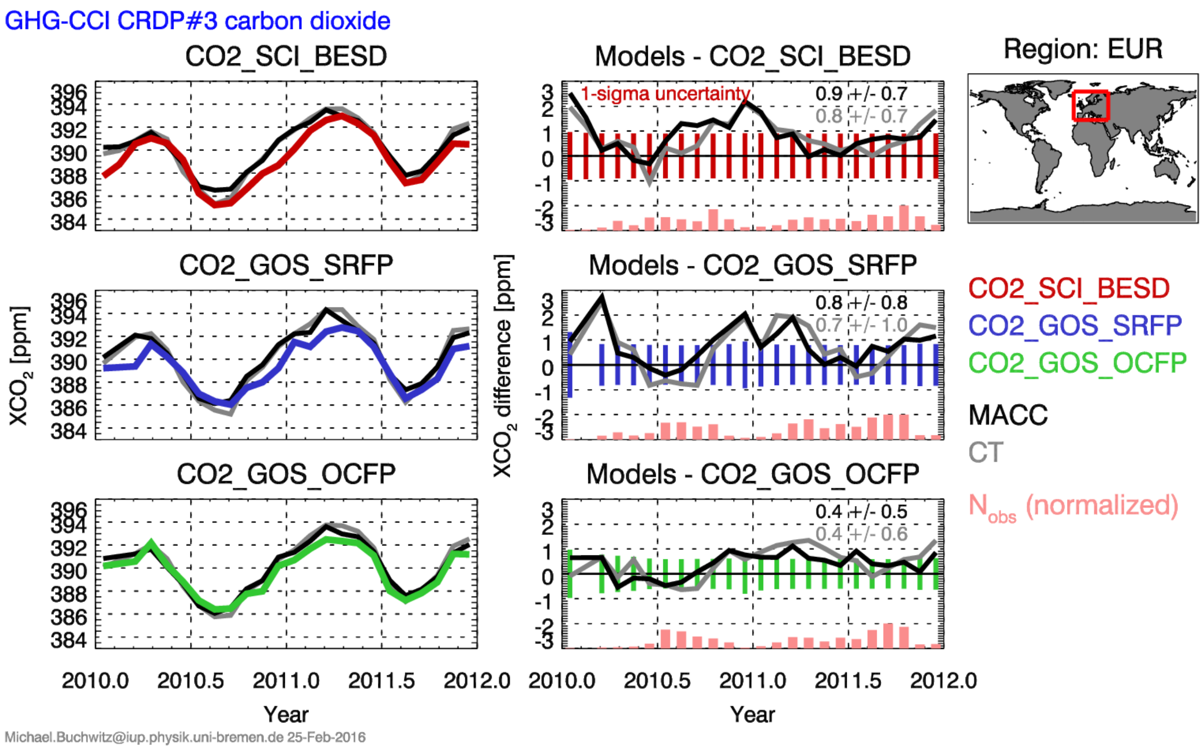

Figure 10: As Fig. 7 but for region Europe (EUR).

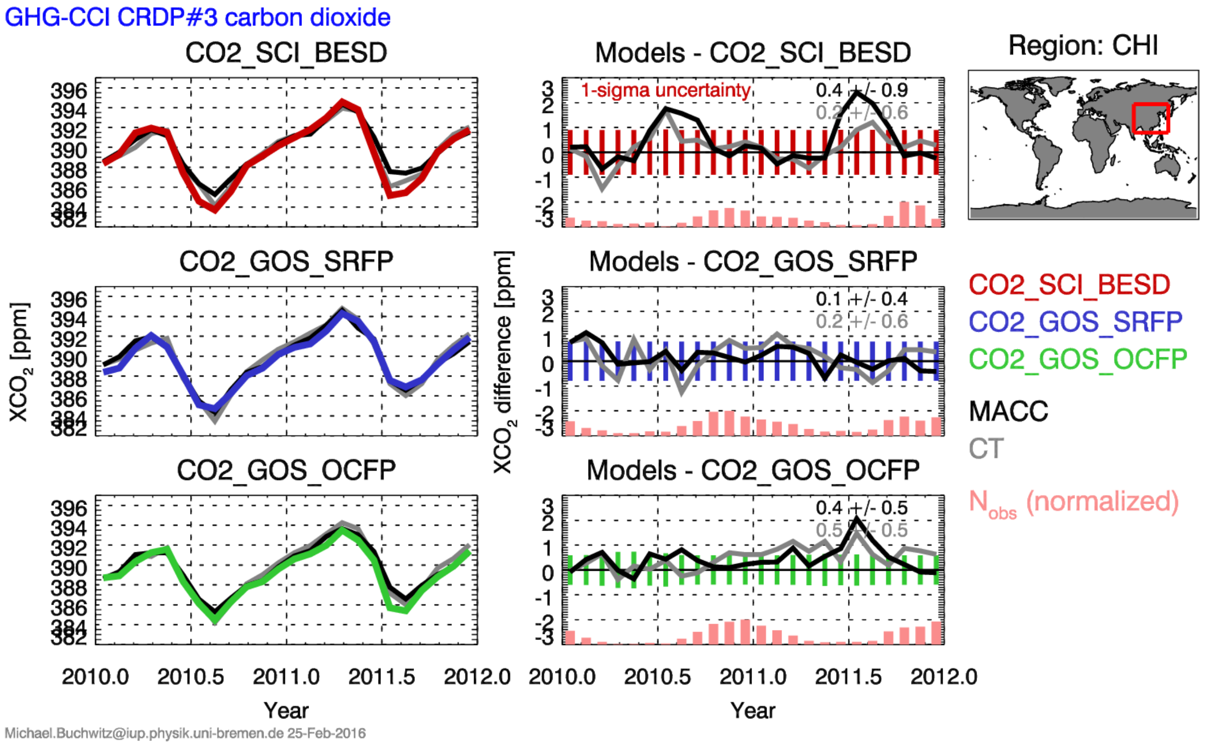

Figure 11: As Fig. 7 but for region China (CHI).

5. XCO_2 error correlations

The GHG-CCI ECA products are Level 2 products, i.e., product information such as XCO_2 and its uncertainty is reported for each individual satellite ground pixel. For applications such as inverse modelling also information on spatio-temporal error correlations would be highly beneficial (see Chevallier et al., 2014b). However, it is not trivial because the needed co-located ground truth observations are only available at TCCON sites, which makes it difficult to obtain reliable global statistics representative for all temporal and spatial distances. Additionally, error correlations may systematically differ depending on surface reflectivity, atmospheric composition (e.g., aerosols and cirrus), viewing geometry and solar illumination conditions. This would violate the assumption of stationarity made by our approach.

Here we report on an attempt to obtain spatio-temporal error correlations in a form useful for inverse modelling and related applications such as CCDAS (Carbon Cycle Data Assimilation Systems (e.g., Kaminski et al., 2013)) (for alternative attempts see Chevallier et al., 2013, and Kulawik et al., 2016). The goal is to obtain a covariance matrix, where each diagonal element corresponds to the variance of the retrieved XCO_2 of a corresponding ground pixel, which is the square of the reported XCO_2 uncertainty, and each non-diagonal element corresponds to the co-variance between two retrievals, i.e., different ground pixels. Our method to estimate co-variances is based on semivariogram analysis (Montero et al., 2015) of the satellite minus TCCON XCO_2 differences. As shown in Reuter et al., 2016, where the analysis method is described in detail, we have used two different parameterizations resulting in a "full" and an "approximate" error covariance matrix. The full error covariance matrix (not shown here; see Reuter et al., 2016, for details) is dense and does not necessarily vanish even for long distances. Therefore, it may be computationally too expensive for many users. A simpler parametrization of the error covariance, whose use can be computationally less demanding, is given by the following formula ("exponential product model"):

$$C_{ij} = \frac{\sigma_i \sigma_j}{V_{max}} \begin{cases} k\ e^{-(\Delta s/l_s + \Delta t/l_t)}, & \Delta s > 0\ or\quad \Delta l > 0 \\ V_{max}, & \Delta s = 0\ and\ \Delta l = 0 \end{cases} \qquad \text{Eq. (3)}$$

Here, σ_i and σ_j correspond to the reported uncertainties for ground pixels *i* and *j* and Δs and Δt are their corresponding spatial (in km) and temporal (in days) differences, respectively. These uncertainties σ are related to the uncertainties reported in the BESDv02.01.01 product files, $\tilde{\sigma}$, by $\sigma = \tilde{\sigma} * 0.2741 + 1.3294$ ppm. V_{max} , k, l_s and l_t are parameters obtained via model semivariogram least squares fitting. Parameter V_{max} (in semivariogram analyses often called "sill", see, e.g., the textbook of Montero et al., 2015) corresponds to the error variance due to all error components. Parameter k is the variance due to correlated errors. The difference V_{max} - k (in semivariogram analyses often called "nugget", see, e.g., the textbook of Montero et al., 2015) corresponds to the fully uncorrelated part of the error, e.g., due to instrumental noise. Parameter l_s is the spatial correlation length and l_t is the temporal correlation length. As shown in Reuter et al., 2016, the following values have been obtained for the

CO2_SCI_BESD product: V_{max} = 3.80 +/- 0.05 ppm^2; k = 1.16 +/- 0.27 ppm^2; l_s = 1476 +/- 633 km and l_t = 58 +/- 20 days (see Fig. 12). Equation 3 and its corresponding parameters has been derived based on relatively coarse assumptions (see Reuter et al., 2016, for details) and future analysis may result in a better approximation but for now we recommend that users who would like to or have to take error correlations into account use the results presented here.

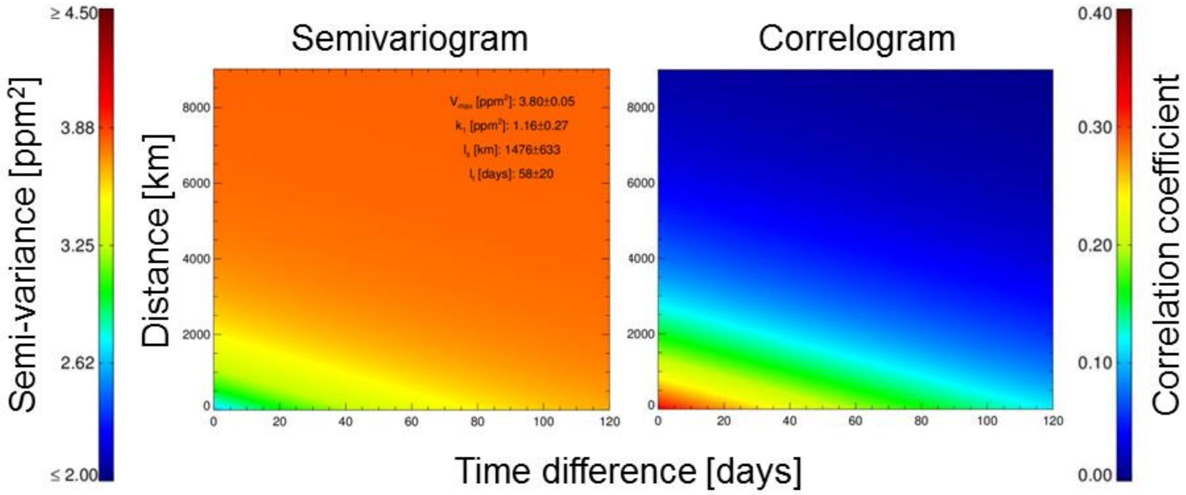

Figure 12: Modelled semivariogram (left; with the four fit parameters listed top right) and corresponding correlogram (right) for product CO2_SCI_BESD. The correlogram, ρ, has been obtained from the semivariogram, γ, via $\rho = 1 - \gamma/V_{max}$. The covariance matrix, C (see Eq. (3)), and the correlogram, ρ, are related by $\rho = C/V_{max}$.

6. XCH_4 global maps and time series

Finally we present some comparisons of global maps of XCH_4 ECA products (Figs. 13a – 13d). Note that many detailed figures for each month and each product (including number of observations per grid cell, standard deviation, etc.) and latitude-resolved time series for the CRDP3 products are shown on the GHG-CCI website (see XCH_4 (and XCO_2) CRDP3 “browse images” on http://www.esa-ghg-cci.org/) and detailed assessment results are presented in several technical documents (e.g., Buchwitz et al., 2016).

Figure 13a shows a global composite map of product CH4_SCI_WFMD for the years 2003-2004, i.e., for the first two years of the GHG-CCI ECA time series at 2°x2° resolution. A major feature is the north-south methane gradient, with higher concentrations over the northern hemisphere, where most of the methane sources are located. Clearly visible by higher regional XCH_4 values are major methane source regions such as China (wetland and rice paddy emissions). However, we have to point out that it is not trivial (if not impossible) to draw clear conclusions with respect to regional emissions from maps such as those shown in Fig 13a due to temporal sampling issues (depending on month, the satellite data may be quite sparse) combined with atmospheric transport and the long lifetime of CH_4 in the atmosphere. For example, large values over water (Fig. 13a) are typically not due to local sources but due to outflow from major source regions (e.g., Asia) located on land.

Figure 13b shows the corresponding map for product CH4_SCI_IMAP. As can be seen, this product is limited to observations over land. The spatial XCH_4 pattern is similar compared to WFMD (Fig. 13a) but not identical. This is due to differences in spatio-temporal sampling of the satellite data, different random errors (see Tab. 7), differences in altitude sensitivity but also due to (different) biases in the satellite data products.

Figures 13c and 13d show global maps for the two GOSAT products CH4_GOS_SRFP (Fig. 13c) and CH4_SCI_OCPR (Fig. 13d) for 2013-2014, i.e., for the two last years of the CRDP3 ECA data set. Both products show similar (but not identical) coverage and pattern, for similar reasons as explained above for the two SCIAMACHY products. Note that detailed comparison and assessment results are shown in Buchwitz et al., 2016, and other technical documents available on the GHG-CCI website (http://www.esa-ghg-cci.org/) and we recommend that users interested in these data products take the information given in these documents into account when using our data products for any given application.

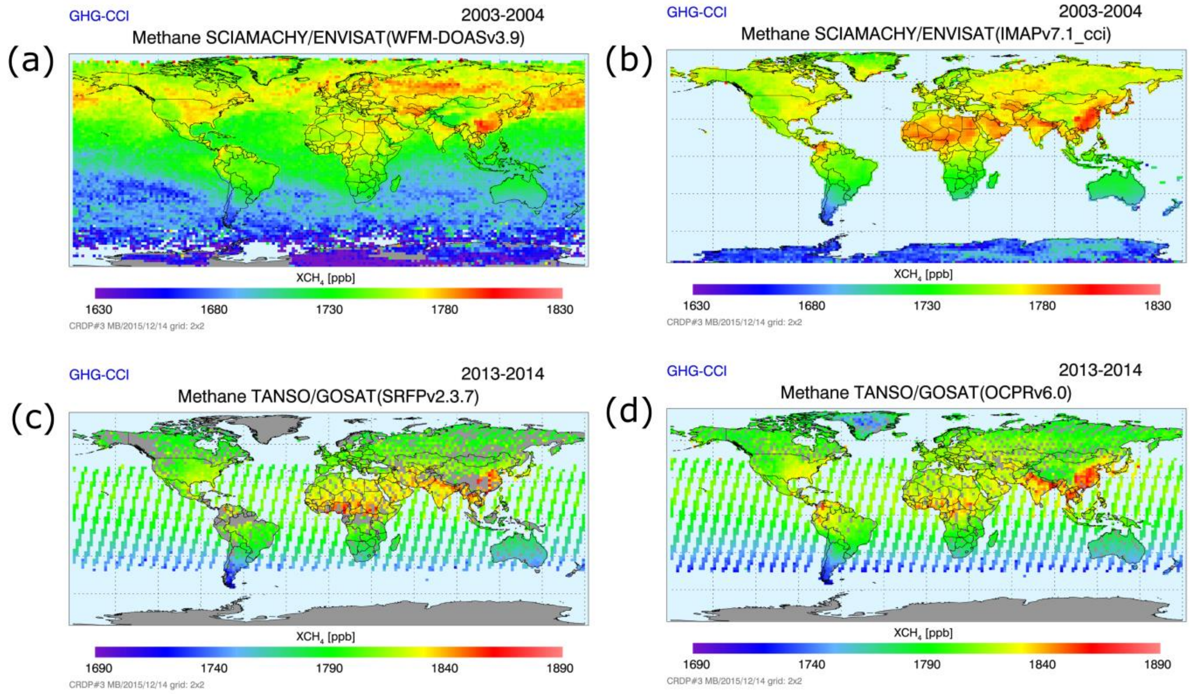

Figure 13: Global maps of satellite-derived XCH_4. (a) Global map of product CH4_SCI_WFMD obtained by gridding all individual retrievals during 2003-2004 using 2^ox2^o grid cells. (b) As (a) but for product CH4_SCI_IMAP. (c) As (a) but for CH4_GOS_SRFP during 2013-2014. (d) As (c) but for CH4_GOS_OCPR. Note the change of the color scale (+ 60 ppb) for the 2013-2014 maps, i.e., for (c) and (d).

7. Summary and conclusions

CO_2 and CH_4 are the two most important greenhouse gases emitted by mankind and responsible for a large fraction of the observed global warming. Despite their importance our knowledge on their various variable surface sources and sinks has significant gaps. Satellite observations of atmospheric CO_2 and CH_4 are increasingly being used to help closing relevant knowledge gaps. We have presented a short overview based on peer-reviewed publications to demonstrate the progress which has been made in recent years concerning the use of satellite retrievals of near-surface-sensitive column-averaged dry air mole fractions of CO_2 and CH_4, i.e., XCO_2 and XCH_4. Nevertheless, much more still needs to be learned about the sources and sinks of these greenhouse gases but this requires additional efforts in terms of further improving the quality of the satellite retrievals, to extend their time series (using existing and future sensors) and to further improve transport modelling and inversion methods as well as more and better satellite and non-satellite observations (e.g., Ciais et al., 2014).

Here we have presented a new XCO_2 and XCH_4 satellite-derived data set called "Climate Research Data Package" No. 3 (CRDP3) which has been generated within the ESA CCI project GHG-CCI. The data products are available for all interested users from the website of this project (http://www.esa-ghg-cci.org/).

The presented XCO_2 and XCH_4 data sets cover the time period end of 2002 – 2014 and have been derived from the nadir near-infrared / shortwave-infrared (NIR/SWIR) radiance observations of the two satellite instruments SCIAMACHY/ENVISAT (2002 - 2012) and TANSO/GOSAT (launched 2009). We have presented time series and global maps including comparisons with TCCON (Wunch et al., 2010, 2011) ground-based observations (version GGG2014) and global CO_2 assimilation system ("models") data sets (European MACC/CAMS model (v14r2) (Chevallier et al., 2015) and NOAA's CarbonTracker (version CT2013B) (Peters et al., 2007)).

Based on validation using TCCON data at six sites we have shown that with one exception the satellite XCO_2 products have (relative) systematic errors of less than 1 ppm, i.e., they meet the Global Climate Observing System (GCOS) accuracy requirement. All XCO_2 products are very stable showing no significant long-term linear trend and they meet the GCOS stability requirement of better than 0.2 ppm/year.

The GOSAT XCH_4 retrievals also meet the GCOS accuracy requirement of better than 10 ppb and are even close to meeting the GHG-CCI breakthrough requirement of better than 5 ppb. These products are also very stable showing no significant long-term linear trend and they meet the GCOS stability requirement of better than 2 ppb/year. For the SCIAMACHY XCH_4 products the situation is more complex due to detector degradation. In particular for 2010 and later years this results in significant biases (not meeting the GCOS accuracy requirement of better than 10 ppb) and large scatter.

The SCIAMACHY BESD XCO_2 and the two GOSAT XCO_2 products (SRON/KIT's SRFP ("RemoTeC") product and University of Leicester's OCFP product) have been compared with output from the MACC model and NOAA's CarbonTracker (CT). Detailed comparison results are presented in terms of global maps and time series for selected regions. Overall it can be concluded that the CO_2 models agree with the satellite retrievals within typically 1-2 ppm but depending on region and time period differences can also be somewhat larger. The two model data sets are very similar, in particular when averaged over large regions, but we also identified significant differences between them. For example, CT shows significantly lower XCO_2 compared to MACC (approximately 4 ppm) over large parts of eastern Russia during summer (JJA season) with MACC being in better agreement with the satellite data compared to CT. Over parts of Amazonia and southern Africa during autumn (SON season) MACC is about 2 ppm higher than CT and over India MACC is about 2-3 ppm lower. For India the satellite data are in better agreement with CT compared to MACC but for Amazonia and southern Africa the situation is less clear. We also identified significant differences between the satellite data products, e.g., a high or a low bias of SRFP compared to other satellite products depending on region and time period. Because the link between atmospheric concentrations and surface fluxes is typically complex our analysis does not necessarily permit to draw clear conclusions on which satellite data set gives the most reliable surface fluxes when used in an inverse modelling framework. This underlines the importance of using multiple satellite products and inversion methods in order to draw robust conclusions on GHG sources and sinks as aimed at in several recent publications (e.g., Chevallier et al., 2013, 2016; Reuter et al., 2014a; Houweling et al., 2015; Feng et al., 2016).

Furthermore, we have presented an attempt to provide users with information on spatio-temporal error correlations using a parameterization of an error covariance matrix obtained via semivariogram analysis of satellite minus TCCON XCO_2 differences. We have also presented global XCH_4 maps to illustrate how the various new XCH_4 products “look like”. Finally, we would like to point out that additional information in terms of various technical documents and separate figures is available on the website of the GHG-CCI project (http://www.esa-ghg-cci.org/) (please note in particular the link to “CRDP (Data)”).

Acknowledgements

This study has been funded by ESA via the GHG-CCI project of ESA’s Climate Change Initiative (CCI). We thank ESA/DLR for providing us with SCIAMACHY Level 1 data products and JAXA for GOSAT Level 1B data. We also thank ESA for making these GOSAT products available via the ESA Third Party Mission archive. We also thank the TCCON team (in particular P. Wennberg, CalTech) for providing TCCON data (obtained via http://tccon.ornl.gov), the European MACC/CAMS projects for providing CO_2 model fields (obtained from http://macc.copernicus-atmosphere.eu/) and NOAA/ESRL for providing CarbonTracker data (obtained via http://www.esrl.noaa.gov/gmd/ccgg/carbontracker/).

1. References

Alexe, M., Bergamaschi, P., Segers, A., et al. (2015), Inverse modeling of CH_4 emissions for 2010–2011 using different satellite retrieval products from GOSAT and SCIAMACHY, *Atmos. Chem. Phys.*, 15, 113–133, www.atmos-chem-phys.net/15/113/2015/, doi:10.5194/acp-15-113-2015.

Basu, S., Guerlet, S., Butz, A., et al. (2013), Global CO_2 fluxes estimated from GOSAT retrievals of total column CO_2, *Atmos. Chem. Phys.*, 13, 8695-8717.

Basu, S., Krol, M., Butz, A., et al. (2014), The seasonal variation of the CO_2 flux over Tropical Asia estimated from GOSAT, CONTRAIL and IASI, *Geophys. Res. Lett.*, doi: 10.1002/2013GL059105.

Bergamaschi, P., Frankenberg, C., Meirink, J.F., Krol, M., Dentener, F., Wagner, T., Platt, U., Kaplan, J.O., Körner, S., Heimann, M., Dlugokencky, E.J., Goede, A. (2007), Satellite chartography of atmospheric methane from SCIAMACHY onboard ENVISAT: 2. Evaluation based on inverse model simulations, *J. Geophys. Res*., 112, D02304, doi:10.1029/2006JD007268.

Bergamaschi, P., Frankenberg, C., Meirink, J. F., Krol, M., Villani, M. G., Houweling, S., Dentener, F., Dlugokencky, E. J., Miller, J. B., Gatti, L. V., Engel, A., Levin, I. (2009), Inverse modeling of global and regional CH_4 emissions using SCIAMACHY satellite retrievals, J. *Geophys. Res.,* 114, D22301, doi:10.1029/2009JD01228.

Bergamaschi, P., Houweling, H., Segers, A., et al. (2013), Atmospheric CH_4 in the first decade of the 21st century: Inverse modeling analysis using SCIAMACHY satellite retrievals and NOAA surface measurements, *J. Geophys. Res*., 118, 7350-7369, doi:10.1002/jrgd.5048.

Bösch, H., Baker, D., Connor, B., Crisp, D., and Miller, C. (2011), Global Characterization of CO_2 Column Retrievals from Shortwave-Infrared Satellite Observations of the Orbiting Carbon Observatory-2 Mission, *Radio Sci*., 3, 270–304, doi:10.3390/rs3020270.

Bloom, A. A., Palmer, P. I., Fraser, A., Reay, D. S., Frankenberg, C. (2010), Large-scale controls of methanogenesis inferred from methane and gravity spaceborne data, *Science*, 327, 322–325, doi:10.1126/science.1175176.

Bovensmann, H., Burrows, J. P., Buchwitz, M., Frerick, J., Noël, S., Rozanov, V. V., Chance, K. V., Goede, A. H. P. (1999), SCIAMACHY - Mission objectives and measurement modes, *J. Atmos. Sci.*, 56 (2), 127-150.

Bovensmann, H., M. Buchwitz, J. P. Burrows, M. Reuter, T. Krings, K. Gerilowski, O. Schneising, J. Heymann, A. Tretner, and J. Erzinger (2010), A remote sensing technique for global monitoring of power plant CO_2 emissions from space and related applications, *Atmos. Meas. Tech*., 3, 781-811.

Buchwitz, M., V.V. Rozanov, and J.P. Burrows (2000), A near-infrared optimized DOAS method for the fast global retrieval of atmospheric CH_4, CO, CO_2, H_2O, and N_2O total column amounts from SCIAMACHY Envisat-1 nadir radiances, *J. Geophys. Res*. 105, 15,231-15,245.

Buchwitz, M., de Beek, R., Burrows, J. P., Bovensmann, H., Warneke, T., Notholt, J., Meirink, J. F., Goede, A. P. H., Bergamaschi, P., Körner, S., Heimann, M., Schulz, A. (2005), Atmospheric methane and carbon dioxide from SCIAMACHY satellite data: Initial comparison with chemistry and transport models, *Atmos. Chem. Phys*., 5, 941-962.

Buchwitz, M., Schneising, O., Burrows, J. P., Bovensmann, H., Reuter, M., Notholt, J. (2007), First direct observation of the atmospheric CO_2 year-to-year increase from space, *Atmos. Chem. Phys*., 7, 4249-4256.

Buchwitz, M., M. Reuter, H. Bovensmann, D. Pillai, J. Heymann, O. Schneising, V. Rozanov, T. Krings, J. P. Burrows, H. Boesch, C. Gerbig, Y. Meijer, and A. Loescher (2013), Carbon Monitoring Satellite (CarbonSat): assessment of atmospheric CO_2 and CH_4 retrieval errors by error parameterization, *Atmos. Meas. Tech*., 6, 3477-3500.

Buchwitz, M., Detmers, R., Boesch, H., et al. (2014), Product Specification Document for the GHG-CCI project of ESA's Climate Change Initiative, version 3 (PSDv3), 6. June 2014, (link: http://www.esa-ghg-cci.org/index.php?q=webfm_send/160).

Buchwitz, M., M. Reuter, O. Schneising, H. Boesch, S. Guerlet, B. Dils, I. Aben, R. Armante, P. Bergamaschi, T. Blumenstock, H. Bovensmann, D. Brunner, B. Buchmann, J. P. Burrows, A. Butz, A. Chédin, F. Chevallier, C. D. Crevoisier, N. M. Deutscher, C. Frankenberg, F. Hase, O. P. Hasekamp, J. Heymann, T. Kaminski, A. Laeng, G. Lichtenberg, M. De Mazière, S. Noël, J. Notholt, J. Orphal, C. Popp, R. Parker, M. Scholze, R. Sussmann, G. P. Stiller, T. Warneke, C. Zehner, A. Bril, D. Crisp, D. W. T. Griffith, A. Kuze, C. O'Dell, S. Oshchepkov, V. Sherlock, H. Suto, P. Wennberg, D. Wunch, T. Yokota, Y. Yoshida (2015), The Greenhouse Gas Climate Change Initiative (GHG-CCI): comparison and quality assessment of near-surface-sensitive satellite-derived CO_2 and CH_4 global data sets, *Remote Sensing of Environment*, 162, 344-362, doi:10.1016/j.rse.2013.04.024.

Buchwitz, M., Dils, B., Boesch, H., Crevoisier, C., Detmers, D., Frankenberg, C., Hasekamp, O., Hewson, W., Laeng, A., Noël, S., Notholt, J., Parker, R., Reuter, M., Schneising, O. (2016), ESA Climate Change Initiative (CCI) Product Validation and Intercomparison Report (PVIR) for the Essential Climate Variable (ECV) Greenhouse Gases (GHG) for data set Climate Research Data Package No. 3 (CRDP#3), Version 4.0, 24. Feb. 2016 (link: http://www.esa-ghg-cci.org/?q=webfm_send/300).

Burrows, J. P., Hölzle, E., Goede, A. P. H., Visser, H., and Fricke, W. (1995), SCIAMACHY—Scanning Imaging Absorption Spectrometer for Atmospheric Chartography, *Acta Astronaut*., 35(7), 445–451, doi:10.1016/0094-5765(94)00278-t.

Butz, A., Hasekamp, O.P., Frankenberg, C., Vidot, J., Aben, I. (2010), CH_4 retrievals from space-based solar backscatter measurements: Performance evaluation against simulated aerosol and cirrus loaded scenes, J. Geophys. Res., VOL. 115, D24302, doi:10.1029/2010JD014514.

Butz, A., Guerlet, S., Hasekamp, O., Schepers, D., Galli, A., Aben, I., Frankenberg, C., Hartmann, J.-M., Tran, H., Kuze, A., Keppel-Aleks, G., Toon, G., Wunch, D., Wennberg, P., Deutscher, N., Griffith, D., Macatangay, R. , Messerschmidt, J., Notholt, J. , Warneke, T. (2011), Towards accurate CO_2 and CH_4 observations from GOSAT, *Geophys. Res. Lett.,* Geophys. Res. Lett., doi:10.1029/2011GL047888.

Butz, A., Galli, A., Hasekamp, O., Landgraf, J., Tol, P., Aben, I. (2012), Remote Sensing of Environment, TROPOMI aboard Sentinel-5 Precursor : Prospective performance of CH_4 retrievals for aerosol and cirrus loaded atmospheres, 120, 267-276, doi:10.1016/j.rse.2011.05.030.

Canadell, J. G., Ciais, P., Dhakal, S., Dolman, H., Friedlingstein, P., Gurney. K. R,, Held, A., Jackson, R. B., Le Quéré, C., Malone, E. L., Ojima, D. S., Patwardhan, A., Peters, G. P., Raupach, M.

R. (2010), Interactions of the carbon cycle, human activity, and the climate system: a research portfolio, *Current Opinion in Environmental Sustainability*, 2, 301–311.

Chevallier, F., Feng, L., Bösch, H., Palmer, P. I., Rayner, P. J. (2010), On the impact of transport model errors for the estimation of CO_2 surface fluxes from GOSAT observations, *Geophys. Res. Lett.*, 37, L21803, doi:10.1029/2010GL044652.

Chevallier, F., and O'Dell, C. W. (2013), Error statistics of Bayesian CO_2 flux inversion schemes as seen from GOSAT, *Geophys. Res. Lett.*, doi: 10.1002/grl.50228.

Chevallier, F., Palmer, P.I., Feng, L., Boesch, H., O'Dell, C.W., Bousquet, P. (2014a), Towards robust and consistent regional CO_2 flux estimates from in situ and space-borne measurements of atmospheric CO_2, *Geophys. Res. Lett.*, 41, 1065-1070, DOI: 10.1002/2013GL058772.

Chevallier, F., Buchwitz, M., Bergamaschi, et al. (2014b), User Requirements Document for the GHG-CCI project of ESA's Climate Change Initiative, version 2 (URDv2), 28. August 2014, (link: http://www.esa-ghg-cci.org/?q=webfm_send/173).

Chevallier, F. (2015), On the statistical optimality of CO_2 atmospheric inversions assimilating CO_2 column retrievals, *Atmos. Chem. Phys.*, 15, 11133–11145.

Chevallier, F., M. Alexe, P. Bergamaschi, D. Brunner, L. Feng, S. Houweling, T. Kaminski, W. Knorr, T. T. van Leeuwen, J. Marshall, P. I. Palmer, M. Scholze, A.-M. Sundström, M. Voßbeck (2016), ESA Climate Change Initiative (CCI) Climate Assessment Report (CAR) for Climate Research Data Package No. 3 (CRDP#3) of the Essential Climate Variable (ECV) Greenhouse Gases (GHG), Version 3, pp. 94, 3 May 2016 (link: http://www.esa-ghg-cci.org/?q=webfm_send/318).

Ciais, P., Dolman, A. J., Bombelli, A., et al. (2014), Current systematic carbon cycle observations and needs for implementing a policy-relevant carbon observing system, *Biogeosciences*, 11, 3547-3602, www.biogeosciences.net/11/3547/2014/, doi:10.5194/bg-11-3547-2014.

Cogan, A. J., Boesch, H., Parker, R. J., et al. (2012), Atmospheric carbon dioxide retrieved from the Greenhouse gases Observing SATellite (GOSAT): Comparison with ground-based TCCON observations and GEOS-Chem model calculations, *J. Geophys. Res*., 117, D21301, doi:10.1029/2012JD018087.

Cressot, C., F. Chevallier, P. Bousquet, et al. (2014), On the consistency between global and regional methane emissions inferred from SCIAMACHY, TANSO-FTS, IASI and surface measurements, *Atmos. Chem. Phys*., 14, 577-592.

Crevoisier, C., Chédin, A., Matsueda, H., Machida, T., Armante, R., Scott, N. A. (2009a), First year of upper tropospheric integrated content of CO_2 from IASI hyperspectral infrared observations, *Atmos. Chem. Phys*., 9, 4797–4810.

Crevoisier, C., Nobileau, D., Fiore, A., Armante, R., Chédin, A., Scott, N. A. (2009b), Tropospheric methane in the tropics – first year from IASI hyperspectral infrared observations, *Atmos. Chem. Phys*., 9, 6337–6350.

Crevoisier, C., D. Nobileau, R. Armante, L. Crépeau, T. Machida, Y. Sawa, H. Matsueda, T. Schuck, T. Thonat, J. Pernin, N. A. Scott, and A. Chédin (2013), The 2007–2011 evolution of tropical methane in the mid-troposphere as seen from space by MetOp-A/IASI, *Atmos. Chem. Phys*., 13, 4279-4289.

Crisp, D., Atlas, R. M., Bréon, F.-M., Brown, L. R., Burrows, J. P., Ciais, P., Connor, B. J., Doney, S. C., Fung, I. Y., Jacob, D. J., Miller, C. E., O'Brien, D., Pawson, S., Randerson, J. T., Rayner, P., Salawitch, R. J., Sander, S. P., Sen, B., Stephens, G. L., Tans, P. P., Toon, G. C., Wennberg, P. O., Wofsy, S. C., Yung, Y. L., Kuang, Z., Chudasama, B., Sprague, G., Weiss, B., Pollock, R., Kenyon, D., and Schroll, S. (2004), The Orbiting Carbon Observatory (OCO) mission, *Adv. Space Res*., 34, 700–709, doi:10.1016/j.asr.2003.08.062.

Crisp, D., Fisher, B. M., O'Dell, C., Frankenberg, C., Basilio, R., Boesch, H. L. R. Brown, R. Castano, B. Connor, N. M. Deutscher, A. Eldering, D. Griffith, M. Gunson, A. Kuze, L. Mandrake, J. McDuffie, J. Messerschmidt, C. E. Miller, I. Morino, V. Natraj, J. Notholt, D. M. O'Brien, F. Oyafuso, I. Polonsky, J. Robinson, R. Salawitch, V. Sherlock, M. Smyth, H. Suto, T. E. Taylor, D. R. Thompson, P. O.Wennberg, D.Wunch, Y. L. Yung (2012), The ACOS CO_2

retrieval algorithm – Part II: Global XCO_2 data characterization, *Atmos. Meas. Tech*., 5, 687–707.

Deng, F., Jones, D. B. A., Henze, D. K., Bousserez, N., Bowman, K. W., Fisher, J. B., Nassar, R., O'Dell, C., Wunch, D., Wennberg, P. O., Kort, E. A., Wofsy, S. C., Blumenstock, T., Deutscher, N. M., Griffith, D. W. T., Hase, F., Heikkinen, P., Sherlock, V., Strong, K., Sussmann, R., and Warneke, T. (2014), Inferring regional sources and sinks of atmospheric CO_2 from GOSAT XCO2 data, *Atmos. Chem. Phys*., 14, 3703-3727, doi:10.5194/acp-14-3703-2014.

Deutscher, N., J. Notholt, J. Messerschmidt, C. Weinzierl, T. Warneke, C. Petri, P. Grupe, K. Katrynski (2014), TCCON data from Bialystok, Poland, Release GGG2014R1. TCCON data archive, hosted by the Carbon Dioxide Information Analysis Center, Oak Ridge National Laboratory, Oak Ridge, Tennessee, U.S.A., http://dx.doi.org/10.14291/tccon.ggg2014.bialystok01.R1/1183984.

Detmers, R. G., O. Hasekamp, I. Aben, S. Houweling, T. T. van Leeuwen, A. Butz, J. Landgraf, P. Koehler, L. Guanter, and B. Poulter (2015), Anomalous carbon uptake in Australia as seen by GOSAT, *Geophys. Res. Lett*., 42, doi:10.1002/2015GL065161.

Dils, B., M. Buchwitz, M. Reuter, O. Schneising, H. Boesch, R. Parker, S. Guerlet, I. Aben, T. Blumenstock, J. P. Burrows, A. Butz, N. M. Deutscher, C. Frankenberg, F. Hase, O. P. Hasekamp, J. Heymann, M. De Maziere, J. Notholt, R. Sussmann, T. Warneke, D. Griffith, V. Sherlock, and D. Wunch (2014), The Greenhouse Gas Climate Change Initiative (GHG-CCI): comparative validation of GHG-CCI SCIAMACHY/ENVISAT and TANSO-FTS/GOSAT CO_2 and CH_4 retrieval algorithm products with measurements from the TCCON, *Atmos. Meas. Tech.*, 7, 1723-1744.

Dils, B., et al. (2016), The GHG-CCI XCO_2 and XCH_4 CRDP3 data set: Comparative validation of global satellite observations with measurements from the TCCON, *this issue, manuscript in preparation*.

Dlugokencky, E. J., Bruhwiler, L., White, J. W. C., Emmons, L. K., Novelli, P. C., Montzka, S. A., Masarie, K. A., Lang, P. M., Crotwell, A. M., Miller, J. B., Gatti, L. V. (2009), Observational constraints on recent increases in the atmospheric CH_4 burden, *Geophys. Res. Lett.*, 36, L18803, doi:10.1029/2009GL039780.

Dlugokencky, E. and Tans, P. (2015), Trends in atmospheric carbon dioxide, National Oceanic & Atmospheric Administration, Earth System Research Laboratory (NOAA/ESRL), available at: http://www.esrl.noaa.gov/gmd/ccgg/trends, last access: 7 October 2015.

Feng, L., P. I. Palmer, R. J. Parker, N. M. Deutscher, D. G. Feist, R. Kivi, I. Morino, and R. Sussmann (2016), Estimates of European uptake of CO_2 inferred from GOSAT XCO_2 retrievals: sensitivity to measurement bias inside and outside Europe, *Atmos. Chem. Phys*., 16, 1289-1302, doi:10.5194/acp-16-1289-2016.

Foucher, P. Y., Chédin, A., Dufour, G., Capelle, V., Boone, C. D., Bernath, P. (2009), Technical Note: Feasibility of CO_2 profile retrieval from limb viewing solar occultation made by the ACE-FTS instrument, *Atmos. Chem. Phys*., 9, 2873–2890.

Frankenberg, C., Meirink, J. F., van Weele, M., Platt, U., Wagner, T. (2005), Assessing methane emissions from global spaceborne observations, *Science*, 308, 1010–1014.

Frankenberg, C., Aben, I., Bergamaschi, P., Dlugokencky, E. J., van Hees, R., Houweling, S., van der Meer, P., Snel, R., Tol, P. (2011), Global column-averaged methane mixing ratios from 2003 to 2009 as derived from SCIAMACHY: Trends and variability, *J. Geophys. Res*., doi:10.1029/2010JD014849.

Fraser, A., Palmer, P. I., Feng, L., et al. (2013), Estimating regional methane surface fluxes: the relative importance of surface and GOSAT mole fraction measurements, *Atmos. Chem. Phys*., 13, 5697-5713, doi:10.5194/acp-13-5697-2013.

Fraser, A., Palmer, P. I., Feng, L., et al. (2014), Estimating regional fluxes of CO_2 and CH_4 using space-borne observations of XCH4:XCO2, *Atmos. Chem. Phys*., 14, 12883-12895, www.atmos-chem-phys.net/14/12883/2014/, doi:10.5194/acp-14-12883-2014.

GCOS (2011), Global Climate Observing System: SYSTEMATIC OBSERVATION REQUIREMENTS FOR SATELLITE-BASED DATA PRODUCTS FOR CLIMATE - 2011 Update - Supplemental details to the satellite-based component of the “Implementation Plan for the Global Observing System for Climate in Support of the UNFCCC (2010 Update)”, GCOS-154.

Griffith, D. W. T., N. Deutscher, V. A. Velazco, P. O. Wennberg, Y. Yavin, G. Keppel Aleks, R. Washenfelder, G. C. Toon, J.-F. Blavier, C. Murphy, N. Jones, G. Kettlewell, B. Connor, R. Macatangay, C. Roehl, M. Ryczek, J. Glowacki, T. Culgan, G. Bryant (2014a), TCCON data from Darwin, Australia, Release GGG2014R0. TCCON data archive, hosted by the Carbon Dioxide Information Analysis Center, Oak Ridge National Laboratory, Oak Ridge, Tennessee, U.S.A., http://dx.doi.org/10.14291/tccon.ggg2014.darwin01.R0/1149290.

Griffith, D. W. T., V. A. Velazco, N. Deutscher, C. Murphy, N. Jones, S. Wilson, R. Macatangay, G. Kettlewell, R. R. Buchholz, M. Riggenbach (2014b), TCCON data from Wollongong, Australia, Release GGG2014R0. TCCON data archive, hosted by the Carbon Dioxide Information Analysis Center, Oak Ridge National Laboratory, Oak Ridge, Tennessee, U.S.A., http://dx.doi.org/10.14291/tccon.ggg2014.wollongong01.R0/1149291.

Guerlet, S., Basu, S., Butz, A., et al. (2013), Reduced carbon uptake during the 2010 Northern Hemisphere summer from GOSAT, *Geophys. Res. Lett*., doi: 10.1002/grl.50402.

Heymann, J., O. Schneising, M. Reuter, M. Buchwitz, V. V. Rozanov, V. A. Velazco, H. Bovensmann, and J. P. Burrows (2012a), SCIAMACHY WFM-DOAS XCO_2: comparison with CarbonTracker XCO_2 focusing on aerosols and thin clouds, Atmos. Meas. Tech., 5, 1935-1952.

Heymann, J., H. Bovensmann, M. Buchwitz, J. P. Burrows, N. M. Deutscher, J. Notholt, M. Rettinger, M. Reuter, O. Schneising, R. Sussmann, and T. Warneke (2012b), SCIAMACHY WFM-DOAS XCO_2: reduction of scattering related errors, *Atmos. Meas. Tech.*, 5, 2375-2390.

Heymann, J., M. Reuter, M. Hilker, M. Buchwitz, O. Schneising, H. Bovensmann, J. P. Burrows, A. Kuze, H. Suto, N. M. Deutscher, M. K. Dubey, D. W. T. Griffith, F. Hase, S. Kawakami, R. Kivi, I. Morino, C. Petri, C. Roehl, M. Schneider, V. Sherlock, R. Sussmann, V. A. Velazco, T. Warneke, and D. Wunch (2015), Consistent satellite XCO_2 retrievals from SCIAMACHY and GOSAT using the BESD algorithm, *Atmos. Meas. Tech*., 8, 2961-2980.

Hollmann, R., Merchant, C. J., Saunders, R., et al. (2013), The ESA Climate Change Initiative: satellite data records for essential climate variables, *Bulletin of the American Meteorological Society* (BAMS), 0.1175/BAMS-D-11-00254.1.

Houweling, S., M. Krol, P. Bergamaschi et al. (2014), A multi-year methane inversion using SCIAMACHY, accounting for systematic errors using TCCON measurements, *Atmos. Chem. Phys*., 14, 3991-4012, http://www.atmos-chem-phys.net/14/3991/2014/, doi:10.5194/acp-14-3991-2014.

Houweling, S., D. Baker, S. Basu, H. Boesch, A. Butz, F. Chevallier, F. Deng, E. J. Dlugokencky, L. Feng, A. Ganshin, O. Hasekamp, D. Jones, S. Maksyutov, J. Marshall, T. Oda, C.W. O'Dell1, S. Oshchepkov, P. I. Palmer, P. Peylin, Z. Poussi, F. Reum, H. Takagi, Y. Yoshida, and R. Zhuravlev (2015), An intercomparison of inverse models for estimating sources and sinks of CO_2 using GOSAT measurements, *J. Geophys. Res*. Atmos., 120, 5253–5266, doi:10.1002/2014JD022962.

IPCC (2013), Climate Change 2013: The Physical Science Basis, Working Group I Contribution to the Fifth Assessment Report of the Intergovernmental Report on Climate Change, http://www.ipcc.ch/report/ar5/wg1/, 2013.

Kaminski, T., W. Knorr, G. Schürmann, M. Scholze, P. J. Rayner, S. Zaehle, S. Blessing, W. Dorigo, V. Gayler, R. Giering, N. Gobron, J. P. Grant, M. Heimann, A. Hooker-Strout, S. Houweling, T. Kato, J. Kattge, D. Kelley, S. Kemp, E. N. Koffi, C. Köstler, P.P. Mathieu, B. Pinty, C. H. Reick, C. Rödenbeck, R. Schnur, K. Scipal, C. Sebald, T. Stacke, A. Terwisscha van Scheltinga, M. Vossbeck, H. Widmann, and T. Ziehn (2013), The BETHY/JSBACH Carbon

Cycle Data Assimilation System: experiences and challenges. *J. Geophys. Res*., 118:doi:10.1002/jgrg.20118.

Kim, J., Kim, H. M., Cho, C.-H., Boo, K.-O., Jacobson, A. R., Sasakawa, M., Machida, T., Arshinov, M., and Fedoseev, N. (2016), Impact of Siberian observations on the optimization of surface CO_2 flux, *Atmos. Chem. Phys. Discuss*., doi:10.5194/acp-2015-875, 2016.

Kirschke, S., Bousquet, P., Ciais, P., et al. (2013), Three decades of global methane sources and sinks, *Nat. Geosci*., 6, 813–823, doi:10.1038/ngeo1955.

Kort, E. A., C. Frankenberg, C. E. Miller, and T. Oda (2012), Space-based observations of megacity carbon dioxide, *Geophys. Res. Lett*., 39, L17806, doi:10.1029/2012GL052738.

Kort, E. A., Frankenberg, C., Costigan, K. R., et al. (2014), Four corners: The largest US methane anomaly viewed from space, *Geophys. Res. Lett*., 41, doi:10.1002/2014GL061503.

Kulawik, S., D. Wunch, C. O'Dell, C. Frankenberg, M. Reuter, T. Oda, F. Chevallier, V. Sherlock, M. Buchwitz, G. Osterman, C. E. Miller, P. O. Wennberg, D. Griffith, I. Morino, M. K. Dubey, N. M. Deutscher, J. Notholt, F. Hase, T. Warneke, R. Sussmann, J. Robinson, K. Strong, M. Schneider, M. De Mazière, K. Shiomi, D. G. Feist, L. T. Iraci, J. Wolf (2016), Consistent evaluation of ACOS-GOSAT, BESD-SCIAMACHY, CarbonTracker, and MACC through comparisons to TCCON, *Atmos. Meas. Tech*., 9, 683-709, doi:10.5194/amt-9-683-2016.

Kuze, A., Suto, H., Nakajima, M., and Hamazaki, T. (2009), Thermal and near infrared sensor for carbon observation Fourier-transform spectrometer on the Greenhouse Gases Observing Satellite for greenhouse gases monitoring, *Appl. Opt*., 48, 6716–6733.

Kuze, A., Taylor, T., Kataoka, F., Bruegge, C., Crisp, D., Harada, M., Helmlinger, M., Inoue, M., Kawakami, S., Kikuchi, N., Mitomi, Y., Murooka, J., Naitoh, M., O’Brien, D., O’Dell, C., Ohyama, H., Pollock, H., Schwandner, F., Shiomi, K., Suto, H., Takeda, T., Tanaka, T., Urabe, T., Yokota, T., and Yoshida, Y. (2014), Long-term vicarious calibration of GOSAT short-wave sensors: techniques for error reduction and new estimates of radiometric degradation factors, *IEEE T. Geosci. Remote*, 52, 3991–4004, doi:10.1109/TGRS.2013.2278696.

Laeng, A., J. Plieninger, T. von Clarmann, U. Grabowski, G. Stiller, E. Eckert, N. Glatthor, F. Haenel, S. Kellmann, M. Kiefer, A. Linden, S. Lossow, L. Deaver, A. Engel, M. Hervig, I. Levin, M. McHugh, S. Noël, G. Toon, and K. Walker, Validation of MIPAS IMK/IAA methane profiles, *Atmos. Meas. Tech.*, 8, 5251-5261, 2015.

Le Quéré, C., Moriarty, R., Andrew, R. M., et al. (2015), Global carbon budget 2015, *Earth Syst. Sci. Data*, 7, 349–396, www.earth-syst-sci-data.net/7/349/2015/, doi:10.5194/essd-7-349-2015.

Lindqvist, H., C. W. O'Dell, S. Basu,3, H. Boesch, F. Chevallier, N. Deutscher, L. Feng, B. Fisher, F. Hase, M. Inoue, R. Kivi, I. Morino, P. I. Palmer, R. Parker, M. Schneider, R. Sussmann, and Y. Yoshida (2015), Does GOSAT capture the true seasonal cycle of XCO_2?, *Atmos. Chem. Phys.*, 15, 13023-13040, doi:10.5194/acp-15-13023-2015, 2015.

Maksyutov, S., H. Takagi, V. K. Valsala, M. Saito, T. Oda1, T. Saeki, D. A. Belikov, R. Saito, A. Ito, Y. Yoshida, I. Morino, O. Uchino, R. J. Andres, and T. Yokota (2013), Regional CO_2 flux estimates for 2009–2010 based on GOSAT and ground-based CO_2 observations, *Atmos. Chem. Phys.*, 13, 9351–9373.

Masarie, K. A., Peters, W., Jacobson, A. R., and Tans, P. P. (2014), ObsPack: a framework for the preparation, delivery, and attribution of atmospheric greenhouse gas measurements, *Earth Syst. Sci. Data*, 6, 375-384, doi:10.5194/essd-6-375-2014.

Massart, S., A. Agustí-Panareda, J. Heymann, M. Buchwitz, F. Chevallier, M. Reuter, M. Hilker, J. P. Burrows, N. M. Deutscher, D. G. Feist, F. Hase, R. Sussmann, F. Desmet, M. K. Dubey, D. W. T. Griffith, R. Kivi, C. Petri, M. Schneider, V. A. Velazco (2016), Ability of the 4-D-Var analysis of the GOSAT BESD XCO_2 retrievals to characterize atmospheric CO_2 at large and synoptic scales, *Atmos. Chem. Phys.*, 16, 1653-1671, doi:10.5194/acp-16-1653-2016.

Monteil, G., Houweling, S., Butz, A., et al. (2013), Comparison of CH_4 inversions based on 15 months of GOSAT and SCIAMACHY observations, *J. Geophy. Res.*, doi: 10.1002/2013JD019760, Vol 118, Issue 20, 11807-11823.

Montero, J. M., Fernandez-Aviles, G., Mateu, J. (2015), Spatial and Spatio-Temporal Geostatistical Modeling and Kriging: John Wiley & Sons Inc., (URL: http://www.ebook.de/de/product/20651121/jose_maria_ montero_gema_fernandez_aviles_jorge_mateu_spatial_and_spatio_ temporal_geostatistical_modeling_and_kriging.html).

Nisbet, E., Dlugokencky, E., Bousquet, P. (2014), Methane on the rise – again, *Science*, 343, 493–495, doi:10.1126/science.1247828.

Noël, S., Bramstedt, K., Rozanov, A., Bovensmann, H., Burrows, J. P. (2011), Stratospheric methane profiles from SCIAMACHY solar occultation measurements derived with onion peeling DOAS, *Atmos. Meas. Tech*., 4, 2567-2577.

Noël,S., K. Bramstedt, M. Hilker, P. Liebing, J. Plieninger, M. Reuter, A. Rozanov, H. Bovensmann, and J. P. Burrows (2016), Stratospheric CH_4 and CO_2 profiles derived from SCIAMACHY solar occultation measurements, *Atmos. Meas. Tech.*, 9, 1485-1503, doi:10.5194/amt-9-1485-2016.

Notholt, J., Dils, B., Blumenstock, T., Brunner, D., Buchmann, B., De Mazière, M., et al. (2012). Product Validation and Algorithm Selection Report (PVASR) of the GHG-CCI project of ESA's Climate Change Initiative. Technical Report, link: http://www.esa-ghg-cci.org/?q=webfm_send/314.

Notholt, J., C. Petri, T. Warneke, N. Deutscher, M. Buschmann, C. Weinzierl, R. Macatangay, P. Gruppe (2014), TCCON data from Bremen, Germany, Release GGG2014R0. TCCON data archive, hosted by the Carbon Dioxide Information Analysis Center, Oak Ridge National Laboratory, Oak Ridge, Tennessee, U.S.A., http://dx.doi.org/10.14291/tccon.ggg2014.bremen01.R0/1149275.

O'Dell, C. W., Connor, B., Boesch, H., et al. (2012), The ACOS CO_2 retrieval algorithm – Part 1: Description and validation against synthetic observations, *Atmos. Meas. Tech.*, 5, 99–121.

Oshchepkov, S., Bril, A., Maksyutov, S., Yokota, T. (2011), Detection of optical path in spectroscopic space-based observations of greenhouse gases: Application to GOSAT data processing, *J. Geophys. Res*., 116, D14304, doi:10.1029/2010JD015352.

Oshchepkov, S., Bril, A., Yokota, T., et al. (2013), Effects of atmospheric light scattering on spectroscopic observations of greenhouse gases from space. Part 2: Algorithm intercomparison in the GOSAT data processing for CO_2 retrievals over TCCON sites, *J. Geophys. Res*., 118, 1493–1512, doi:10.1002/jgrd.50146.

Pandey, S., S. Houweling, M. Krol, I. Aben, F. Chevallier, E. J. Dlugokencky, L. V. Gatti, E. Gloor, J. B. Miller, R. Detmers, T. Machida, T. Roeckmann (2016), Inverse modeling of GOSAT-retrieved ratios of total column CH_4 and CO_2 for 2009 and 2010, Atmos. Chem. Phys., 16, 5043–5062, doi:10.5194/acp-16-5043-2016.

Parazoo, N. C., Bowman, K., Frankenberg, C., et al. (2013), Interpreting seasonal changes in the carbon balance of southern Amazonia using measurements of XCO_2 and chlorophyll fluorescence from GOSAT, *Geophys. Res. Lett*., 40, 2829–2833, doi:10.1002/grl.50452.

Parker, R., Boesch, H., Cogan, A., Fraser, A., Feng, L, Palmer, P., Messerschmidt, J., Deutscher, N., Griffth, D., Notholt, J., Wennberg, P. Wunch, D. (2011), Methane Observations from the Greenhouse gases Observing SATellite: Comparison to ground-based TCCON data and Model Calculations, *Geophys. Res. Lett*., doi:10.1029/2011GL047871.

Parker, R. J., H. Boesch, K. Byckling, A. J. Webb, P. I. Palmer, L. Feng, P. Bergamaschi, F. Chevallier, J. Notholt, N. Deutscher, T. Warneke, F. Hase, R. Sussmann, S. Kawakami, R. Kivi, D. W. T. Griffith, and V. Velazco (2015), Assessing 5 years of GOSAT Proxy XCH_4 data and associated uncertainties, *Atmos. Meas. Tech*., 8, 4785-4801, doi:10.5194/amt-8-4785-2015.

Peters, W., Jacobson, A. R., Sweeney, C., Andrews, A. E., Conway, T. J., Masarie, K., Miller, J. B., Bruhwiler, L. M. P., Petron, G., Hirsch, A. I., Worthy, D. E. J., van der Werf, G. R., Randerson, J. T., Wennberg, P. O., Krol, M. C., Tans, P. P. (2007): An atmospheric perspective on North American carbon dioxide exchange: CarbonTracker, *Proceedings of the*

National Academy of Sciences (*PNAS*) of the United States of America, 27 Nov. 2007, 104(48), 18925-18930.

Peylin, P., Law, R. M., Gurney, et al. (2013), Global atmospheric carbon budget: results from an ensemble of atmospheric CO_2 inversions, *Biogeosciences*, 10, 6699–6720, doi:10.5194/bg-10-6699-2013, URL http://www.biogeosciences.net/10/6699/2013/.

Reuter, M., Buchwitz, M., Schneising, O., Heymann, J., Bovensmann, H., Burrows, J. P. (2010), A method for improved SCIAMACHY CO_2 retrieval in the presence of optically thin clouds, *Atmos. Meas. Tech*., 3, 209-232.

Reuter, M., Bovensmann, H., Buchwitz, M., Burrows, J. P., Connor, B. J., Deutscher, N. M., Griffith, D. W. T., Heymann, J., Keppel-Aleks, G., Messerschmidt, J., Notholt, J., Petri, C., Robinson, J., Schneising, O., Sherlock, V., Velazco, V., Warneke, T., Wennberg, P. O., Wunch, D. (2011), Retrieval of atmospheric CO_2 with enhanced accuracy and precision from SCIAMACHY: Validation with FTS measurements and comparison with model results, *J. Geophys. Res*., 116, D04301, doi:10.1029/2010JD015047.

Reuter, M., H. Boesch, H. Bovensmann, A. Bril, M. Buchwitz, A. Butz, J. P. Burrows, C. W. O'Dell, S. Guerlet, O. Hasekamp, J. Heymann, N. Kikuchi, S. Oshchepkov, R. Parker, S. Pfeifer, O. Schneising, T. Yokota, and Y. Yoshida (2013), A joint effort to deliver satellite retrieved atmospheric CO_2 concentrations for surface flux inversions: the ensemble median algorithm EMMA, *Atmos. Chem. Phys*., 13, 1771-1780.

Reuter, M., Buchwitz, M., Hilker, M., et al. (2014a), Satellite-inferred European carbon sink larger than expected, *Atmos. Chem. Phys*., 14, 13739-13753, www.atmos-chem-phys.net/14/13739/2014/, doi:10.5194/acp-14-13739-2014.

Reuter, M., Buchwitz, M., Hilboll, A., et al. (2014b), Decreasing emissions of NOx relative to CO_2 in East Asia inferred from satellite observations, *Nature Geoscience*, 28 Sept. 2014, doi:10.1038/ngeo2257, pp.4.

Reuter, M., Hilker, M., Schneising, O., Buchwitz, M., Heymann (2016), J., ESA Climate Change Initiative (CCI) Comprehensive Error Characterisation Report: BESD full-physics retrieval algorithm for XCO_2 for the Essential Climate Variable (ECV) Greenhouse Gases (GHG), Version 2.0, revision 1, 10.02.2016 (pdf file: http://www.esa-ghg-cci.org/webfm_send/284).

Rigby, M., Prinn, R. G., Fraser, P. J., Simmonds, P. G., Langenfelds, R. L., Huang, J., Cunnold, D. M., Steele, L. P., Krummel, P. B., Weiss, R. F., O'Doherty, S., Salameh, P. K., Wang, H. J., Harth, C. M., Mühle, J., Porter, L. W. (2008), Renewed growth of atmospheric methane, *Geophys. Res. Lett*., 35, L22805, doi:10.1029/2008GL036037.

Rodgers, C. D. (2000), Inverse Methods for Atmospheric Sounding: Theory and Practice, *World Scientific Publishing*.

Ross, A. N., Wooster, M. J., Boesch, H., Parker, R. (2013), First satellite measurements of carbon dioxide and methane emission ratios in wildfire plumes, *Geophys. Res. Lett*., 40, 1-5, doi:10.1002/grl.50733.

Saeki, T., Maksyutov, S., Saito, M., Valsala, V., Oda, T., Andres, R. J., Belikov, D., Tans, P., Dlugokencky, E., Yoshida, Y., Morino, I., Uchino, O., and Yokota, T. (2013), Inverse modeling of CO_2 fluxes using GOSAT data and multi-year ground-based observations, *Sci. Online Lett. Atmos*., 9, 45–50, doi:10.2151/sola.2013-011.

Schaefer, H., S. E. Mikaloff Fletcher, C. Veidt, K. R. Lassey, G. W. Brailsford, T. M. Bromley, E. J. Dlugokencky, S. E. Michel, J. B. Miller, I. Levin, D. C. Lowe, R. J. Martin, B. H. Vaughn, J. W. C. White (2016), A 21st-century shift from fossil-fuel to biogenic methane emissions indicated by $^{13}CH_4$, *Science*, Vol. 352, Issue 6281, pp. 80-84, doi 10.1126/science.aad2705.

Schepers, D., Guerlet, S., Butz, A., Landgraf, J., Frankenberg, C., Hasekamp, O., Blavier, J.-F., Deutscher, N. M., Griffith, D. W. T., Hase, F., Kyro, E., Morino, I., Sherlock, V., Sussmann, R., Aben, I. (2012), Methane retrievals from Greenhouse Gases Observing Satellite (GOSAT) shortwave infrared measurements: Performance comparison of proxy and physics retrieval algorithms, *J. Geophys. Res*., 117, D10307, doi:10.1029/2012JD017549.

Schneising, O., Buchwitz, M., Burrows, J. P., Bovensmann, H., Reuter, M., Notholt, J., Macatangay, R., Warneke, T. (2008), Three years of greenhouse gas column-averaged dry air mole fractions retrieved from satellite - Part 1: Carbon dioxide, *Atmos. Chem. Phys*., 8, 3827-3853.

Schneising, O., Buchwitz, M., Burrows, J. P., Bovensmann, H., Bergamaschi, P., Peters, W. (2009), Three years of greenhouse gas column-averaged dry air mole fractions retrieved from satellite - Part 2: Methane, *Atmos. Chem. Phys*., 9, 443-465.

Schneising, O., Buchwitz, M., Reuter, M., Heymann, J., Bovensmann, H., and Burrows, J. P. (2011), Long-term analysis of carbon dioxide and methane column-averaged mole fractions retrieved from SCIAMACHY, *Atmos. Chem. Phys*., 11, 2881-2892.

Schneising, O., Bergamaschi, P., Bovensmann, H., Buchwitz, M., Burrows, J. P., Deutscher, N. M., Griffith, D. W. T., Heymann, J., Macatangay, R., Messerschmidt, J., Notholt, J., Rettinger, M., Reuter, M., Sussmann, R., Velazco, V. A., Warneke, T., Wennberg, P. O., Wunch, D. (2012), Atmospheric greenhouse gases retrieved from SCIAMACHY: comparison to ground-based FTS measurements and model results, *Atmos. Chem. Phys*., 12, 1527-1540.

Schneising, O., Heymann, J., Buchwitz, M., Reuter, M., Bovensmann, H., and Burrows, J. P. (2013), Anthropogenic carbon dioxide source areas observed from space: assessment of regional enhancements and trends, *Atmos. Chem. Phys*., 13, 2445-2454.

Schneising, O., Reuter, M., Buchwitz, M., Heymann, J., Bovensmann, H., and Burrows, J. P. (2014a), Terrestrial carbon sink observed from space: variation of growth rates and seasonal cycle amplitudes in response to interannual surface temperature variability, *Atmos. Chem. Phys*., 14, 133-141.

Schneising, O., Burrows, J. P.,, Dickerson, R. R., Buchwitz, M., Reuter, M., Bovensmann, H. (2014b), Remote sensing of fugitive methane emissions from oil and gas production in North American tight geologic formations, *Earth's Future*, 2, DOI: 10.1002/2014EF000265, pp. 11.

Schulze, E. D., Luyssaert, S., Ciais, P, et al. (2009), Importance of methane and nitrous oxide emissions for Europe's terrestrial greenhouse gas balance, *Nat. Geosci*., 2, 842–850, doi:10.1038/ngeo686.

Shindell, D. T., Pechony, O., Voulgarakis, A., et al. (2013), Interactive ozone and methane chemistry in GISS-E2 historical and future climate simulations, *Atmos. Chem. Phys*., 13, 2653–2689, doi:10.5194/acp-13-2653-2013.

Stephens, B. B., Gurney, K. R., Tans, P. P., Sweeney, C., Peters, W., Bruhwiler, L., Ciais, P., Ramonet, M., Bousquet, P., Nakazawa, T., Aoki, S., Machida, T., Inoue, G., Vinnichenko, N., Lloyd, J., Jordan, A., Heimann, M., Shibistova, O., Langenfelds, R. L., Steele, L. P., Francey, R. J., Denning, A. S. (2007), Weak northern and strong tropical land carbon uptake from vertical profiles of atmospheric CO*2*, *Science*, 22, 1732–1735.

Sussmann, R., Forster, F., Rettinger, M., and Bousquet, P. (2012), Renewed methane increase for five years (2007-2011) observed by solar FTIR spectrometry, *Atmos. Chem. Phys*., 12, 4885-4891.

Takagi, H., S. Houweling, R. J. Andres, D. Belikov, A. Bril, H. Boesch, A. Butz, S. Guerlet, O. Hasekamp, S. Maksyutov, I. Morino1, T. Oda, C. W. O'Dell, S. Oshchepkov, R. Parker, M. Saito, O. Uchino, T. Yokota, Y. Yoshida, V. Valsala (2014), Influence of differences in current GOSAT XCO_2 retrievals on surface flux estimation, *Geophys. Res. Lett*., 41, 2598–2605, doi:10.1002/2013GL059174.

Turner, A. J., D. J. Jacob, K. J. Wecht, J. D. Maasakkers, S. C. Biraud, H. Boesch, K. W. Bowman, N. M. Deutscher, M. K. Dubey, D. W. T. Griffith, F. Hase, A. Kuze, J. Notholt, H. Ohyama, R. Parker, V. H. Payne, R. Sussmann, V. A. Velazco, T. Warneke, P. O. Wennberg, and D. Wunch (2015), Estimating global and North American methane emissions with high spatial resolution using GOSAT satellite data, *Atmos. Chem. Phys*., 15, 7049-7069, doi:10.5194/acp-15-7049-2015.

Turner, A. J., D. J. Jacob, J. Benmergui, S. C. Wofsy, J. D. Maasakkers, A. Butz, O. Hasekamp, and S. C. Biraud (2016), A large increase in U.S. methane emissions over the past decade inferred from satellite data and surface observations, *Geophys. Res. Lett.*, 43, 2218–2224, doi:10.1002/2016GL067987.

Veefkind, J. P., Aben, I., McMullan, K., Förster, H., De Vries, J., Otter, G., Claas, J., Eskes, H. J., De Haan, J. F., Kleipool, Q., Van Weele, M., Hasekamp, O., Hoogeveen, R., Landgraf, J., Snel, R., Tol, P.,Ingmann, P., Voors, R., Kruizinga, B., Vink, R., Visser, H., and Levelt, P. F. (2012), TROPOMI on the ESA Sentinel-5 Precursor: A GMES mission for global observations of the atmospheric composition for climate, air quality and ozone layer applications. *Rem. Sens. Environment*, 120:70–83.

Velazco, V. A., M. Buchwitz, H. Bovensmann, M. Reuter, O. Schneising, J. Heymann, T. Krings, K. Gerilowski, and J. P. Burrows (2011), Towards space based verification of CO_2 emissions from strong localized sources: fossil fuel power plant emissions as seen by a CarbonSat constellation, *Atmos. Meas. Tech.*, 4, 2809-2822.

Wecht, K. J, Jacob, D. J., Sulprizio, M. P., et al. (2014), Spatially resolving methane emissions in California: constraints from the CalNex aircraft campaign and from present (GOSAT, TES) and future (TROPOMI, geostationary) satellite observations, *Atmos. Chem. Phys.*, 14, 8173-8184, www.atmos-chem-phys.net/14/8173/2014/, doi:10.5194/acp-14-8173-2014.

Wennberg, P. O., C. Roehl, D. Wunch, G. C. Toon, J.-F. Blavier, R. Washenfelder, G. Keppel-Aleks, N. Allen, J. Ayers., (2014a), TCCON data from Park Falls, Wisconsin, USA, Release GGG2014R0. TCCON data archive, hosted by the Carbon Dioxide Information Analysis Center, Oak Ridge National Laboratory, Oak Ridge, Tennessee, U.S.A., http://dx.doi.org/10.14291/tccon.ggg2014.parkfalls01.R0/1149161.

Wennberg, P. O., D. Wunch, C. Roehl, J.-F. Blavier, G. C. Toon, N. Allen, P. Dowell, K. Teske, C. Martin, J. Martin (2014b), TCCON data from Lamont, Oklahoma, USA, Release GGG2014R0. TCCON data archive, hosted by the Carbon Dioxide Information Analysis Center, Oak Ridge National Laboratory, Oak Ridge, Tennessee, U.S.A., http://dx.doi.org/10.14291/tccon.ggg2014.lamont01.R0/1149159.

Worden, J. R., A. J. Turner, A. Bloom, S. S. Kulawik, J. Liu, M. Lee, R. Weidner, K. Bowman, C. Frankenberg, R. Parker, and V. H. Payne (2015), Quantifying lower tropospheric methane concentrations using GOSAT near-IR and TES thermal IR measurements, doi:10.5194/amt-8-3433-2015, *Atmos. Meas. Tech.*, 8, 3433–3445.

Wunch, D., Toon, G. C., Wennberg, P. O., Wofsy, S. C., Stephens, B. B., Fischer, M. L., Uchino, O., Abshire, J. B., Bernath, P., Biraud, S. C., Blavier, J.-F. L., Boone, C., Bowman, K. P., Browell, E. V., Campos, T., Connor, B. J., Daube, B. C., Deutscher, N. M., Diao, M., Elkins,

J. W., Gerbig, C., Gottlieb, E., Griffith, D. W. T., Hurst, D. F., Jimenez, R., Keppel-Aleks, G., Kort, E. A., Macatangay, R., Machida, T., Matsueda, H., Moore, F., Morino, I., Park, S., Robinson, J., Roehl, C. M., Sawa, Y., Sherlock, V., Sweeney, C., Tanaka, T., Zondlo, M. A. (2010), Calibration of the Total Carbon Column Observing Network using aircraft profile data, *Atmos. Meas. Tech*., 3, 1351–1362, doi:10.5194/amt-3-1351-2010, http://www.atmos-meas-tech.net/3/1351/2010/.

Wunch, D., Toon, G. C., Blavier, J.-F. L., Washenfelder, R. A., Notholt, J., Connor, B. J., Griffith, D. W. T., Sherlock, V., Wennberg, P. O. (2011a), The Total Carbon Column Observing Network, *Phil. Trans. R. Soc. A*, 369, 2087–2112, doi:10.1098/rsta.2010.0240.

Wunch, D., Wennberg, P. O., Toon, G. C., et al. (2011b), A method for evaluating bias in global measurements of CO_2 total columns from space, *Atmos. Chem. Phys*., 11, 12317–12337, www.atmos-chem-phys.net/11/12317/2011/, doi:10.5194/acp-11-12317-2011.

Wunch, D., Toon, G. C., Sherlock, V., Deutscher, N. M, Liu, X., Feist, D. G., and Wennberg, P. O. (2015), The Total Carbon Column Observing Network's GGG2014 Data Version. Carbon Dioxide Information Analysis Center, Oak Ridge National Laboratory, Oak Ridge, Tennessee, USA, available at: doi:10.14291/tccon.ggg2014.documentation.R0/1221662.

Yoshida, Y., Kikuchi, N., Morino, I., et al. (2013), Improvement of the retrieval algorithm for GOSAT SWIR XCO_2 and XCH_4 and their validation using TCCON data, *Atmos. Meas. Tech*., 6, 1533–1547, doi:10.5194/amt-6-1533-2013.

Zhang, Q., R.-L. Shia, S. P. Sander, and Y. L. Yung (2016), XCO_2 retrieval error over deserts near critical surface albedo, *Earth and Space Science*, 3, doi:10.1002/2015EA000143.